ISSN 0029-3865

CNPq

CBPF – CENTRO BRASILEIRO DE PESQUISAS FÍSICAS

Notas de Física

CBPF-NF-059/93

Total Nuclear Photoabsorption Cross Section in the Range 0.2 - 1.0 GeV for Nuclei Throughout the Periodic Table

by

M.L. Terranova and O.A.P. Tavares

Rio de Janeiro
1993

Abstract. An analysis of the total photoabsorption cross section for nuclei ranging from ^{4}He up to ^{238}U has been performed in the energy range 0.2-1.0 GeV. Mean total photoabsorption cross sections have been obtained by summing up the contributions from partial photoreactions, and found to follow an A^{1}-dependence in the 0.2-1.0 GeV range. A review of the available total photoabsorption cross section data is also presented. Comparisons have been made with cross section values calculated by considering both the quasi-deuteron and π-meson photoproduction mechanism of primary nuclear photointeraction.

PACS: 25.20.+y

Key-words: Photonuclear reactions; Nuclear photoabsorption; Photonuclear cross section; Intermediate-energy photons.

1. Introduction

The study of the total photonuclear absorption cross section, $\sigma_{\gamma A}^{T}(k,A)$, of complex nuclei with mass number A≥4 at photon energies above the giant dipole resonance (GDR, k > 20 MeV) has been carried out over the past years in different laboratories [1-26] (see Table 1). The different experimental methods which have been used to obtain the values of $\sigma_{\gamma A}^{T}$ are the photon transmission technique, the photohadronic method, and the detection of cross sections for selected hadronic processes which are considered to exhaust the whole absorption cross section. A detailed description of these methods is given in [27]. Depending on the energy range investigated and on the mass number of the nucleus of interest, detection of part of the photohadronic processes [7,8,18] and of the multi-neutron emission [8, 21,22,24] as well as photofission measurements [2-6,16,23,25] have been performed. Despite the rather large amount of photonuclear data accumulated over the last decade by using monochromatic (or quasi-monochromatic) photons, our knowledge of $\sigma_{\gamma A}^{T}$ is still restricted to a limited number of nuclei and defined photon energy ranges.

At incident photon energies above GDR the nuclear photoabsorption has been currently described by the so-called quasi-deuteron mechanism proposed by Levinger [28,29].This process of nuclear photoabsorption via correlated neutron-proton pairs is the dominant one below the π-meson photoproduction threshold ($k \lesssim 140$ MeV), although at higher energies it still contributes to some extent to the total nuclear photoabsorption.

At energies above 140 MeV the interaction of incident photons with nuclei occurs through excitation of bound nucleons and production of baryon resonance states.

In the range 140<k<400 MeV a rather large body of experimental data on both light and heavy nuclei has led to an A-dependence of the total cross section of the type

$$\sigma_{\gamma A}^{T} \propto A^{b} \quad , \qquad (1)$$

with b ranging between 0.8 [13,14] and 1.1 [18]. Besides, in [22] a linear dependence of $\sigma_{\gamma A}^{T}$ upon A was found, at least for nuclei with masses greater than 150.

At higher energies (k >2 GeV) the hadron-like behaviour of photons and subsequent shadowing effects [30,31] give rise to an A-dependence of the type (1), but with $b < 1$ [32]. A lack of information there exists indeed in the interval 0.4-2.0 GeV, where a not totally well defined experimental situation [8] prevents one from deducing any relationship between $\sigma_{\gamma A}^{T}$ and A.

Prior to the eighties, a great variety of photonuclear reactions on complex nuclei were investigated by using bremsstrahlung of maximum energies up to about 1 GeV as photon sources [33-66]. The reaction yields of these experiments were measured by radiochemical methods (activation analysis of irradiated samples) or, in the case of fission studies, by using dielectric fission-track recorders and nuclear-track emulsion.

The use of the photon-difference method enabled evaluation of the absolute reaction cross section as a function of photon energy. In many instances, however, the reported cross section

represents only mean values referred to the energy interval investigated.

Above the GDR region, photoreaction yields have been currently interpreted in the framework of a two-step interaction model according to which, firstly, a rapid intranuclear cascade develops from collisions and/or reabsorption of photoproduced pions, and/or from scattering of recoil nucleons. During the second reaction stage the excited residual nucleus de-excites by a mechanism of competition between fission and particle-evaporation processes [67,68].

The present work originated from an attempt to evaluate, for a number of nuclei throughout the Periodic Table, the total absorption cross section by summing over the cross sections of the partial photoreactions. For this purpose we collected and handled together the whole set of available photoinduced reaction cross sections in the energy domain 0.2-1.0 GeV. Data obtained with bremsstrahlung photons have been considered as partial contributions of the different de-excitation channels to the total inelastic cross section. This allowed us to obtain an A-dependence of the average total cross section, $\overline{\sigma}_{\mu}^{T}$ (mean value in the energy range considered). Moreover for a number of nuclei the total photoabsorption cross section, $\sigma_{\mu}^{T}(k)$, measured by using monochromatic photons is reported (Table 1) as a function of energy and compared with calculated values.

2. Evaluation of total nuclear photoabsorption cross section from primary photointeractions

In the energy range 0.2-1.0 GeV the incident photon can interact either with individual nucleons or with correlated neutron-proton pairs within the target nucleus. The total photoabsorption cross section is therefore described by the sum of the contributions of the two different interaction mechanisms. For a photon of energy k incident on a target nucleus (Z,A) it is evaluated by

$$\sigma_{\gamma A}^{T}(k,A) = Z\sigma_{\gamma p}^{b}(k) + (A-Z)\sigma_{\gamma n}^{b}(k) + \frac{L(A-Z)Z}{A}\sigma_{\gamma d}^{f}(k)\,. \qquad (2)$$

In (2) $\sigma_{\gamma p}^{b}$ and $\sigma_{\gamma n}^{b}$ represent the total photohadronic cross section for individual "bound" proton and neutron, respectively, i.e., the total photoproduction cross section of free nucleons corrected for binding effects and Fermi-motion; $\sigma_{\gamma d}^{f}$ is the total photodisintegration cross section of the free deuteron, and L is the so-called Levinger's constant which measures the relative probability of two nucleons being near each other in a complex nucleus compared with that in a free deuteron.

2.1. A-dependence of the mean total photoabsorption cross section.

From (2), by averaging over the energy interval 0.2-1.0 GeV, we obtain

$$\overline{\sigma}_{\gamma A}^{T}(A) = Z\overline{\sigma}_{\gamma p}^{b} + (A-Z)\overline{\sigma}_{\gamma n}^{b} + \frac{L(A-Z)Z}{A}\overline{\sigma}_{\gamma d}^{f} \,. \qquad (3)$$

The quantities $\overline{\sigma}_{\gamma p}^{b}$ and $\overline{\sigma}_{\gamma n}^{b}$ have been calculated from the corresponding "free" cross sections taken, respectively, from the papers by Damashek and Gilman [69] and Armstrong et al.[70].

For $\sigma_{\gamma d}^{f}$ we used up to 440 MeV the data compiled by Rossi et al.[71], and above 440 MeV the values measured by Myers et al.[72]. The average values result to be $\overline{\sigma}_{\gamma p}^{b}$ = 260 μb ; $\overline{\sigma}_{\gamma n}^{b}$ = 234 μb ; $\overline{\sigma}_{\gamma d}^{f}$ = 17 μb .

The constant L has been recently evaluated as [73]

$$L = 6.8 - 11.2\, A^{-2/3} + 5.7\, A^{-4/3}. \qquad (4)$$

Finally, by expressing cross section values in mb, we obtain

$$\overline{\sigma}_{\gamma A}^{T}(A) = 0.26(0.10Z + 0.90A) + 0.017L(1 - Z/A)Z \,. \qquad (5)$$

The $\overline{\sigma}_{\gamma A}^{T}(A)$ - values calculated from (5) for all nuclei along the Periodic Table are reported in Fig.1. It is worth noticing that the $\overline{\sigma}_{\gamma A}^{T}(A)$ -values plotted as a function of mass number follow a quite completely linear trend, as evidenced by the result of a least-squares analysis

$$\overline{\sigma}_{\gamma A}^{T}(A) = (0.270 \pm 0.005)\ A \ \text{mb} \qquad (0.2\text{-}1.0\ \text{GeV}). \qquad (6)$$

One can appreciate that for A=1 (proton or neutron)

$\overline{\sigma}_{\gamma n}^{T} \simeq \overline{\sigma}_{\gamma n}^{f}$ (within~10% : cf. [70]), and $\overline{\sigma}_{\gamma p}^{T} \simeq \overline{\sigma}_{\gamma p}^{f}$

(within ~3%: cf. [69]). Moreover, for A=2 (deuteron), (6) gives $\overline{\sigma}_{\gamma d}^{T}$ = 0.540 mb, which value compares quite well with the average value of deuteron total photohadronic cross section measured by Armstrong et al. [70]. In addition , it is seen that the contribution to $\overline{\sigma}_{\gamma A}^{T}$ due to quasi-deuteron mechanism of primary

photointeraction (lower curve) amounts to about 10% in the case of intermediate-mass and heavy nuclei, and drops to 3-6% for the lightest ones.

An interesting feature is shown in Fig.2, where the quantity $\sigma_{\gamma A}^{T}(k,A)/A$ is reported as a function of A at four given photon energy values. As one can see, $\sigma_{\gamma A}^{T}$ also results proportional to A, chiefly at higher energies and for more complex nuclei.

The linear dependence of $\sigma_{\gamma A}^{T}$ on A is seen to hold practically for all nuclei at energies greater than about 400 MeV, and for nuclei with $A \gtrsim 20$ at lower photon energies.

2.2. Variation of total nuclear photoabsorption cross section with photon energy : the " Universal Curve"

In the last decade total photonuclear cross sections above the GDR have been measured for a number of target nuclei by using high-quality monochromatic (or quasi-monochromatic) photon beams (Table 1). These data are currently analysed by considering the quantity $\sigma_{\gamma A}^{T}/A$, i.e., by scaling the measured cross section with the total number of nucleons. It is now well established [4,18,19,24,74,75] that $\sigma_{\gamma A}^{T}$/A-values reported as a function of the photon energy k result rather independent of mass number. The trend of $\sigma_{\gamma A}^{T}(k,A)/A$ vs. k has been reasonably well fitted to the so-called "Universal Curve" proposed by Ahrens [76,77], thus indicating an A^1-dependence of the total absorption cross section in the Δ-resonance region. The "Universal Curve", which has been constructed by averaging the data from

nuclei $7 \leq A \leq 238$ at each photon energy, is reported in Fig.3 (dashed line).

Aiming to compare experimental $\sigma_{\gamma A}^{T}/A$ -values with those calculated from primary photointeraction mechanisms, (2) is re-written as

$$\sigma_{\gamma A}^{T}(k,A)/A = (Z/A)\sigma_{\gamma p}^{b}(k) + (1 - Z/A)\sigma_{\gamma n}^{b}(k) + L(1 - Z/A)(Z/A)\sigma_{\gamma d}^{f}(k) . \qquad (7)$$

By averaging the Z- and A-dependent coefficients in (7) for all nuclei along the beta-stability valley , one obtains

$$\left\langle \frac{\sigma_{\gamma A}^{T}}{A} \right\rangle = \left\langle \frac{Z}{A} \right\rangle \sigma_{\gamma p}^{b}(k) + \left[1 - \langle Z/A \rangle\right]\sigma_{\gamma n}^{b}(k) + \left\langle L\left(1 - \frac{Z}{A}\right)\frac{Z}{A} \right\rangle \sigma_{\gamma d}^{f}(k) , \qquad (8)$$

where

$$\langle Z/A \rangle = 0.43 \pm 0.03 \quad , \quad \langle L(1- Z/A)\ Z/A \rangle = 1.49 \pm 0.12 . \qquad (9)$$

The smooth curve arising from this treatment is depicted in Fig.3 (upper full line with hatched area). This curve represents the expected variation of the total photoabsorption cross section, averaged over the Periodic Table, as a function of energy, and is seen to reproduce rather well the more prominent features of the Δ-resonance (maximum of 510 ± 30 μb at 315 MeV, and width of 240 ± 20 MeV). Also shown in Fig.3 is the trend obtained by disregarding the primary quasi-deuteron photointeraction (lower full line).

The trend defined by (8) allows one to obtain a rough estimate of the total nuclear photoabsorption cross section for a given nucleus through the expression

$$\sigma_{\gamma A}^{T}(k,A) \approx \left\langle \frac{\sigma_{\gamma A}^{T}}{A} \right\rangle \times A \quad . \qquad (10)$$

3. Mean total nuclear photoabsorption cross section from partial photoreactions

From a phenomenological point of view intermediate energy photonuclear reactions can be classified as :

i) simple direct reactions : (γ,n) and (γ,p);

ii) multiple neutron photoproduction : (γ,xn) , x>1 ;

iii) π-meson production : (γ, π^{o}xN), (γ, π^{+}xN) and (γ, π^{-}x N);

iv) spallation reactions: (γ,xpyn) with x$\geq$ 1, y$\geq$ 1 ;

v) fission reactions (γ, F);

vi) fragmentation reactions (γ,fr).

The mean total nuclear photoabsorption cross section in the energy range 0.2-1.0 GeV can therefore be obtained by summing up the contributions arising from all partial reactions i-vi), i.e.;

$$\overline{\sigma}_{\gamma A}^{T} = \overline{\sigma}(\gamma,n) + \overline{\sigma}(\gamma,p) + \overline{\sigma}(\gamma,xn) + \overline{\sigma}(\gamma,\pi xN) + \overline{\sigma}(\gamma,xpyn) + \overline{\sigma}(\gamma,F) + \overline{\sigma}(\gamma,fr) \quad , \tag{11}$$

where the $\bar{\sigma}$'s represent mean values obtained in that energy range.

Cross section measurements analyzed in this Section have been performed by using bremsstrahlung beams [33-66]. The mean cross sections per photon were obtained from the corresponding measured reaction yields. Where not explicitly determined by the authors quoted in the mentioned references, mean partial cross sections have been calculated from the experimental yield curves by a least-squares analysis. In the energy range

investigated, from about 0.2 to about 1 GeV (in most cases 0.3-1.0 GeV) a pure 1/k-dependence of the bremsstrahlung spectra was assumed.

The partial photoreactions listed above, as well as the formulae derived from statistical treatments of the experimental data, are discussed in some details in the following.

3.1. (γ,n) reactions

Reactions in which one neutron is lost from the struck nucleus have been extensively and systematically studied mostly in the energy range 0.3-1.0 GeV (Frascati) and 0.2-0.8 GeV (Lund). A compilation of experimental data can be found in [56].

A least-squares treatment of the data enabled to obtain the relationship [56]

$$\overline{\sigma}(\gamma,n) = 0.104 A^{0.81} \quad mb \,, \tag{12}$$

which gives a reasonably good fit to the mean experimental cross section values.

3.2 (γ,p) reactions

As far as (γ,p) processes are concerned ,only a limited number of experiments have been performed in the energy range of interest. The measured cross sections are affected by large uncertainties. A comprehensive survey of available data is reported in [65]. The cross sections measured in the range 0.2-0.8

GeV were analysed as a function of the number Z of protons in the target nucleus and found satisfactorily reproduced by the equation $\overline{\sigma}(\gamma,p) = 0.115\ Z^{0.5}$ mb. Aiming to evidence the dependence of $\overline{\sigma}(\gamma,p)$ upon mass number A we reanalysed the data, thus obtaining

$$\overline{\sigma}(\gamma, p) = 0.078 A^{0.50} \quad mb \ . \tag{13}$$

3.3. (γ,xn) reactions , x > 1

For a given number x of emitted neutrons, the relationship between mean cross section and mass number has been derived from data taken in the 0.2-1 GeV energy range. The data have been compiled and analysed in [61], which reports

$$\overline{\sigma}_x(\gamma, xn) = 0.187 A^{0.684} \exp\left[-37 A^{-0.924}(x-1)^{5/4}\right] \quad mb \ . \tag{14}$$

The above equation is valid for x ranging from 2 up to x_m, the maximum number of neutrons which can be emitted from a given target nucleus. By assuming a loss of excitation energy of about 10 MeV per evaporated neutron, and by using the average values of nuclear excitation for the post-cascade nucleus calculated by Barashenkov et al.[67], we succeeded in finding the following dependence of x_m on A:

$$x_m \approx 1.4 A^{0.457} \ . \tag{15}$$

For each nucleus under examination the mean total cross section for multiple neutron emission can thus be evaluated by summing up all the partial cross sections for neutron emission from x=2 up to the proper x_m-value, i.e. ,

$$\overline{\sigma}(\gamma, xn) = \sum_{x=2}^{x_m} \sigma_x(\gamma, xn) \quad , x_m \approx 1.4 A^{0.457} \ . \tag{16}$$

It should be noted, however, that (14-16) cannot be used for elements characterized by a low fission barrier, and are, therefore, valid only in the case of nuclei with $A \lesssim 230$.

3.4. Pion photoproduction reactions, (γ, π xN)

Reactions of the type (γ, π^0xN),(γ, π^+xN), and (γ, π^-xN) are now being considered. When x=0 these reactions can be considered as direct reactions in which one π-meson is emitted. In the case of $x \geq 1$ the term x represents the multiplicity of nucleons eventually emitted from the residual nucleus left in an excited state ($E^* > 0$). Unfortunately only few experimental data , regarding moreover partial processes on a limited number of target nuclei, have been reported [33,34,38,39,40,42,49,50,57, 62]. In addition, the energy-ranges investigated rarely cover the 0.2- 1.0 GeV interval.

For the purpose of the present work pion photoproduction cross sections have been estimated by taking advantage of the results of a Monte Carlo calculation [78,79] which yielded reaction probabilities, $\Phi_i(k,A)$, for π^o , π^+ , and π^- production in 12 selected nuclei (from ^{7}Li up to ^{209}Bi) at 15 photon energy values up to 1 GeV . These calculations were performed by taking into account the possibility of the residual nucleus to be left in an excited state.

The cross section of the i-th partial meson photoproduction

reaction is thus written as

$$\sigma_i(k, A) = \Phi_i(k, A)\sigma_{\gamma A}^T(k, A) . \qquad (17)$$

By taking for $\sigma_{\gamma A}^T$ the values already discussed in Section 2, and summing up all reaction probability values, we constructed for the 12 nuclei investigated the curves representing total meson photoproduction cross section as a function of energy. Finally, from these curves we obtained the average cross section values in the range 0.2-1.0 GeV. These data are plotted in Fig.4, which shows in a log-scale a quite completely linear trend. A least-squares treatment gives

$$\overline{\sigma}_i(\gamma, \pi) = 0.027 A^{0.847} \quad mb . \qquad (18)$$

3.5. Spallation reactions, (γ,xpyn)

These are photoinduced reactions in which a residual nucleus, the so-called spallation residual, is produced from the struck nucleus by a nominal loss of x protons ($1 \lesssim x \lesssim Z/2$) and y neutrons ($1 \lesssim y \lesssim (A-Z)/2$). A large amount of experimental data has been accumulated in the past, the region of investigated nuclei ranging from Al to Au. An almost complete list of photo-spallation studies at intermediate energies can be found in the papers by Jonsson and Lindgren [54] and Foshina et al.[80].

For target nuclei with $A \lesssim 90$, spallation cross section data have been systematized by using a standard four-parameter

formula [80] . The formula, which allows one to estimate the mean cross section for the production of a given spallation residual, is written as

$$\overline{\sigma}_{xy}(\gamma, sp) = \sigma_M \exp\left[-B(x-1) - K(x - C\alpha y)^2\right] , \qquad (19)$$

where α is the ratio Z/(A-Z) of the target nucleus, and σ_M, B, K, and C are parameters. The values of the parameters are given by:

$$\left.\begin{array}{ll} \sigma_M = 15.7E^{-1.356} \quad mb , & E \lesssim 21 \text{ MeV} / N \\ \sigma_M = 0.248 \quad mb , & E \gtrsim 21 \text{ MeV}/ N \end{array}\right) \qquad (20)$$

$$\left.\begin{array}{ll} B = 3.03E^{-1.06} . & E \lesssim 10 \text{ MeV}/ N \\ B = 0.25 & E \gtrsim 10 \text{ MeV}/ N \end{array}\right) . \qquad (21)$$

where

$$E = 447/A \quad MeV/N \quad , K = 0.466, C = 2.30\alpha - 1.044 . \qquad (22)$$

In this way the mean total photospallation cross section can be obtained by summing up all partial cross section values, i.e.,

$$\overline{\sigma}_t(\gamma, sp) = \sum_{x=1}^{Z/2} \sum_{y=1}^{(A-Z)/2} \overline{\sigma}_{xy}(\gamma, sp) \quad , A \lesssim 90 . \qquad (23)$$

For nuclei with A$\gtrsim$90 a good estimate of the mean cross section is provided by the photospallation systematics by Jonsson and Lindgren [54]. In the energy range 0.25-1.0 GeV these authors were successfull in describing the isobaric distributions of spallation residuals (A_p, Z_p) by means of Rudstam's five-parameter formula [81]

$$\overline{\sigma}_{Z_p,A_p}(\gamma, sp) = \frac{\sigma_0 APR^{2/3}}{1.79\left[e^{PA}-1\right]} \exp\left[PA_p - R\left|Z_p - SA_p + TA_p^{\,2}\right|^{3/2}\right], \qquad (24)$$

with

$$\begin{aligned} P &= 5.22\,A^{-0.89} \\ R &= 11.8\,A_p^{-0.45} \\ S &= 0.486 \\ T &= 0.00038 \\ \sigma_0 &= 0.3 \quad mb\,. \end{aligned} \qquad (25)$$

Since in (24) the quantity $\sigma_0 A$ represents the total inelastic cross section, in the present analysis we thought it more appropriate to use for σ_0 the value 0.270 mb, which has been obtained by averaging $\sigma_{\gamma A}^{T}$ over the 0.2-1.0 GeV interval (see (6)).

From (24) we thus obtained

$$\overline{\sigma}_{Z_p,A_p}(\gamma, sp) = 4.08\,A^{0.11}A_p^{-0.30} \exp\left[-P(A-A_p) - R\left|Z_p - (SA_p - TA_p^{\,2})\right|^{3/2}\right] \; mb \qquad (26)$$

and hence

$$\overline{\sigma}_t(\gamma, sp) = \sum_{A_p}\sum_{Z_p} \overline{\sigma}_{Z_p,A_p}(\gamma, sp) \qquad , A \gtrsim 90 \qquad . \qquad (27)$$

It has to be noted, however, that formulae (25-27) do not apply to target nuclei with mass number greater than about 170, in view of the fact that for heavy nuclei fission is known to compete with spallation. On the other hand, photofission does predominate for actinide nuclei as a consequence of the low fission barrier. It is not easy to define unambiguously the mass regions where photospallation and photofission reactions take place . One can try to delineate schematically these mass regions

as follows

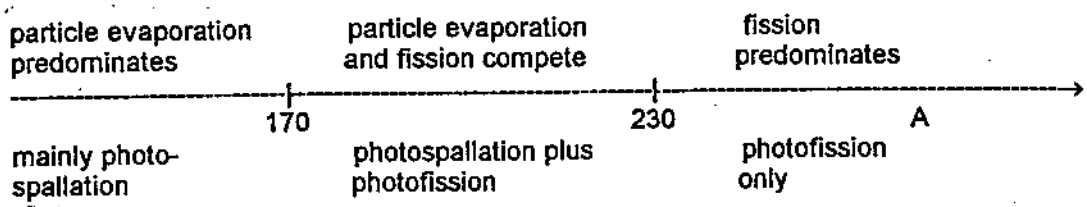

One has to keep in mind that the A-values above reported are only indicative, because the lack of experimental information does not allow the marking of a clear division between the different mass regions. From the above considerations we were led to use formulae (25-27) for the mass range 90-170 only. For A $\gtrsim$230, where the contribution of the spallation process vanishes, only fission data have been considered (see next section).

The trend of $\overline{\sigma}_t(\gamma,sp)$ obtained from (20-23) and (25-27) is shown in Fig.5.

3.6. Photofission reactions, (γ,F)

In the energy range 0.2-1.0 GeV photofission is a process which, depending on the mass region investigated, competes with multineutron photoproduction and photospallation processes. For A $\gtrsim$230 fission is indeed known to exhaust the total inelastic reaction channel.

Despite the large number of photofission experiments reported in the literature, compilations and/or systematics of the available data have not yet been published. The purpose of the present work was to analyse all existing photofission data [1,4,5,16,35-37,41,43-48,51-53,59,60,63,64] covering the target

mass region from ^{56}Fe up to ^{243}Am and the energy range 0.2-1.0 GeV. The mean photofission cross section values are listed in Table 2, and plotted in Fig.6 as a function of parameter Z^2/A. Inspection of the figure reveals two distinct mass regions corresponding to different degrees of contribution of the photofission cross section to the total photoreaction cross section. In the first region ($Z^2/A \gtrsim 30$, $A \gtrsim 185$) where fission contributes either significantly ($30 \leq Z^2/A \lesssim 33$) or predominantly ($Z^2/A \gtrsim 33$), a least-squares treatment of the available data yielded

$$\bar{\sigma}(\gamma,F) = \frac{100}{1+\exp\left[1.125(35.38 - Z^2/A)\right]} \quad mb \quad , \quad \begin{matrix} Z^2/A \gtrsim 30 \\ A \gtrsim 185 \end{matrix} . \qquad (28)$$

In the region $12 \lesssim Z^2/A \lesssim 30$ ($56 \lesssim A \lesssim 185$)) photofission does not contribute significantly to the overall inelastic cross section. In this region , especially in the vicinity of the minimum ($Z^2/A \simeq 23$), photofission can be considered negligible in respect to other photonuclear processes . For nuclei with A ranging between 56 and 185 cross section values have been taken directly from the curve of Fig.6.

3.7. Fragmentation reactions,(γ,fr)

These are reactions in which the splitting of the struck nucleus is accomplished by the emission of aggregates of massive clusters of nucleons. Fragmentation reactions are expected to occur during the fast intranuclear cascade stage of the reaction, as a result of a localized heating of nuclear matter.

Despite the fact that this type of photoreaction has been observed to play a noticeable role at energies above 1GeV or so

[82,83], some indications exist that the fragmentation process would be effective, at least to a low extent, even at photon energies in the range 0.3-1 GeV [55,58,62]. The fragmentation cross sections are of the order of tens of μb, as one can infer from [55,58,62,66].

It is worth noticing that fragmentation events would be distinguished with much difficulty from those due to fission events in experiments performed on intermediate-mass nuclei by using the current methods for detection of nuclear products ,i.e., activation analysis and mica and glass track-detectors. The low cross section values expected for such reactions may be considered at least as partially included in data obtained for other photoinduced processes by the methods mentioned above.

3.8. Sum of the mean cross sections of the partial photoreactions

For nuclei throughout the Periodic Table the mean total nuclear photoabsorption cross section , $\overline{\sigma}^{T}_{\mu}(A)$, can now be obtained from (11) by summing the cross section values for the partial photoreactions discussed in the previous sections. In doing so, it should be remarked that in the mass region $170 \lesssim A \lesssim 230$ there are not clear indications about the relative contributions of the two competing processes, fission and spallation. It was not possible,therefore, to obtain reliable data for nuclei located in that mass region, as well as for thorium.

The final result is shown in Fig.7, where the filled circles represent the $\overline{\sigma}^{T}_{\mu}$ -values obtained for the

different nuclei by means of the above described procedure. The linear dependence of $\overline{\sigma}_{\gamma A}^{T}$ on A, clearly seen in Fig.7, is evidenced by a least-squares analysis which gives the full straight line

$$\overline{\sigma}_{\gamma A}^{T} = (0.28 \pm 0.03) A \quad mb \, . \tag{29}$$

Within the referred uncertainties the above trend rather coincides with $\overline{\sigma}_{\gamma A}^{T} = (0.270 \pm 0.005)$ A mb , which has been evaluated on the basis of the primary photointeraction mechanisms (see (6)).

As a concluding remark we point out that although the mean cross section for some partial photoreactions behaves as A^{α} , $\alpha < 1$, the mean total nuclear cross section exhibits an A^{1}-dependence.

3.9. The behaviour of partial photoreactions throughout the Periodic Table

Results reported in the precedent paragraphs can be used to evaluate the contribution due to photospallation reactions in the mass region $170 \leq A \leq 230$, and hence to study the trend of partial photoreactions throughout the Periodic Table (Fig.8). In the case of spallation reactions it follows from (11) that

$$\overline{\sigma}_{\gamma,sp} = \overline{\sigma}_{\gamma A}^{T} - \sum_{i} \overline{\sigma}_{i} \quad , \quad i = n, p, xn, \pi, F \, , \tag{30}$$

i.e., the mean photospallation yield can be obtained by subtrac-

ting from the mean total reaction yield the sum of all other contributions. This procedure allows one to draw the dashed portion of the spallation curve plotted in Fig.8. The prominent features shown in Fig.8 are briefly remarked hereafter:

i) photospallation is by far the dominant process for intermediate-mass nuclei; it amounts to about 30% of the total mean photoreaction cross section in the region C-Na, and reaches about 70% in the Br-Zr region ; for nuclei with $A \approx 200$ it decreases to about 50%, but for more massive nuclei the contribution arising from spallation drops dramatically;

ii) for heavy nuclei simple-direct processes such (γ,n), (γ,p) and (γ,π) are found altogether to contribute up to 18% ;

iii) (γ,xn) reaction is the second important process occurring in nuclei with $150 \leq A \leq 200$; iv) very light nuclei ($A \leq 10$) are seen to absorb photons through simple-direct processes.

From Fig. 8 it is possible to extract information about the different contributions to the total cross section. As an example, for a target nucleus located in the Co-Ni region we have: photofission 2.6% ; direct (γ,p) reaction 3.4% ; total π-meson photoproduction 5.0% ; multineutron photoproduction 11% ; direct one-neutron photoproduction 16% ; total photoproduction of spallation residuals 62% .

4. Energy-dependence of total photonuclear absorption cross section

This section is devoted to a discussion on total nuclear photoabsorption cross section, $\sigma_{\mu}^{T}(k,A)$, as a function of the incident photon energy, k. Experimental data , expressed as $\sigma_{\mu}^{T}(k,A)/A$, have been reported in Figs.9-16 for ^{4}He, ^{6}Li, ^{7}Li, ^{9}Be, ^{12}C, ^{16}O, ^{27}Al, ^{48}Ti, ^{59}Ni, ^{64}Cu, ^{96}Mo, ^{119}Sn, Pb, ^{235}U, and ^{238}U. Also reported in Figs.9-16 are the corresponding $\sigma_{\mu}^{T}(k,A)/A$ - values calculated by means of (7). These latter in all the figures are represented by full lines. A comparison shows that nearly 45% of the overall data displayed in figures 9-16 agree with calculated values within ~15% or less. The best agreement , not only in individual measurements but also in the cross section trend, is by far verified with data taken for Al, Ti, Cu and Sn by Arends et al.[18].

The measurements for ^{6}Li (Fig.9b) and ^{7}Li (Fig.10a) by the Mainz group [14] reproduce the calculated trends within 20% or less. A satisfactory agreement between measured values and the calculated ones is found for ^{6}Li [14], ^{9}Be [13,10], ^{12}C [9,10,24], ^{16}O [9,18], ^{27}Al [9,18], Ti [18], Cu [18], Sn [18] and Pb [24,18]. For some nuclei (He, Be, C, Pb, ^{235}U, ^{238}U) the values of σ_{μ}^{T}/A measured in the Δ-resonance region (300-320 MeV) differ from the calculated ones by 20-25% .

At higher energies ($k \gtrsim 400$ MeV), good agreement is however found between measured and calculated values in the cases of ^{9}Be [9,10], ^{12}C [9,10,24], ^{16}O [12], ^{27}Al[9], Pb [21,24], ^{235}U

[16,19], and ^{238}U [1,4,16,45], although the cross section trend for these nuclei is not completely reproduced in the entire energy range.

Total photoabsorption cross section measurements by the Khar'kov group [7] result on the contrary somewhat higher as compared with those by other laboratories or with the calculated curves (Figs.11a, 12a, 13a, and 14a).

Finally, data regarding the uranium isotopes should be particularly discussed. Due to their very small values of fission barrier (~5 MeV) the fission cross section for these isotopes is believed to represent the total photoabsorption cross section (see, for instance, [4]). As a consequence, photoabsorption cross sections are currently achieved by measuring photofission cross sections. In Fig.16a-b are displayed the results of fission measurements performed for ^{235}U and ^{238}U isotopes. As one can see, the experimental trends from all laboratories reproduce clearly the resonance-like shape around 320 MeV. Differences exist, however, as far as intensities are concerned, mostly between the measurements carried out with bremsstrahlung beams [1,45,51].

Quite good agreement is indeed observed in Fig.16b when comparing to each other recent data obtained by monochromatic photon beams [4,6,16,19]. At photon energies below ~230 MeV and above ~360 MeV a large number of experimental points is found to reproduce rather well the curve (full line) calculated by summing the contributions due to both quasi-deuteron and photomesonic primary interactions. Such an agreement ,

nevertheless, fails to occur near the peak of the Δ-resonance, where only the data by Wakuta et al.[45] are seen to compare with the calculated trend. This behaviour may be indicative of a damping effect due to the Δ-resonance. One should consider, moreover, that in the energy region of the Δ-resonance other reaction channels begin to play an increasing role for the total photoabsorption process, as already discussed in Section 3.9.

At higher energies ($k \gtrsim 500$ MeV) data taken at Frascati (filled triangles [4]) and Mainz (filled circles [16]) do not provide any indication of a resonance-like shape in the region of the second baryon resonance (~710 MeV). As already pointed out [4,16], this result seems to be indicative of a strong damping effect, not yet completely understood, of the referred resonance. The old bremsstrahlung data [1,45,51] do not allow achievement of precise information in the energy range of the second resonance.

Despite the discrepancies in cross section data from different experimental groups, a resonance-like trend of the total photoabsorption cross section of complex nuclei has been always found around 350 MeV, where the photoabsorption cross section is dominated by the excitation of the Δ-resonance. In this energy region the primary photointeraction via neutron-proton pairs is also expected to contribute to total photonuclear absorption, at least to a lesser extent. It is very difficult , however, to detect experimentally such a contribution. It can be indeed of the same order of magnitude of the uncertainties asso-

ciated with most of the total cross section measurements. On the other hand, at photon energies above the Δ-resonance, both paucity of data and measurement precision does not allow any definite conclusions to be drawn about the features of the higher baryon resonances in complex nuclei.

5. Summary and conclusions

In the course of the present work we reviewed and discussed the total photoabsorption cross section for complex nuclei throught the Periodic Table in the range 0.2-1.0 GeV. Nuclear photoabsorption has been described in the framework of two primary mechanisms, namely, photointeraction with correlated neutron-proton pairs, and excitation of bound nucleons to baryon resonance states (π-meson photoproduction).

In order to investigate the behaviour of the total photoabsorption cross section, averaged over the 0.2-1.0 GeV interval, as a function of mass number, the contributions due to the partial photoreactions have been analysed and summed up. Experimental data used in this analysis were those obtained by means of bremsstrahlung beams.

The resulting mean total photoabsorption cross sections have been found to compare quite well with the calculated ones. This study allowed us to conclude that the mean photoabsorption cross section follows an A^1-dependence, even if the mean cross sections for the partial reactions were not found to follow such a dependence. For light nuclei simple direct processes like the (γ,n) and (γ,p) reactions are seen to predominate, whereas

photospallation results to be the most important reaction for intermediate-mass nuclei. For the heaviest nuclei photofission is by far the dominant mode by which nuclei de-excite following photoabsorption, although the present analysis has indicated that a non-negligible contribution to the total photonuclear cross section comes from direct processes. In this context, we felt it worthwhile to report a compilation of available photofission measurements in the 0.2-1.0 GeV range (Table 2).

On the other hand, the variation of the total photoabsorption cross section with photon energy has been discussed for a number of nuclei from ^{4}He up to ^{238}U. For this study use has been made of recent measurements mostly performed with monochromatic photons ,at Frascati, Novosibirsk, Khar'kov, Yerevan, Mainz, Bonn, Saclay, and Glasgow. Comparisons have been made between calculated and measured total photoabsorption strength per nucleon, σ_{μ}^{T}/A ,which shows a trend rather independent from the mass number for all nuclei investigated. Agreement has been found in many instances between measured and calculated values, either in the Δ-resonance region or at higher energies. Nevertheless, the trend of σ_{μ}^{T}/A is shown not completely reproduced for all nuclei in the entire 0.2-1.0 GeV energy range. One should remark that the contribution to total photoabsorption arising from the primary interaction via neutron-proton pairs is not to be disregarded in the region of Δ-resonance, as one can see from inspection of Fig.3. In the case of ^{238}U the present analysis has indicated that simple direct processes such as (γ,n) reactions are likely to represent a non-negligible contribution to the

total photoreaction channel.

The problem of having reliable sets of measured total photonuclear cross sections at intermediate energies is a very difficult task. Experimental difficulties there still exist when measuring total nuclear photoabsorption. Formulae reported in this paper may be used advantageously to obtain estimates of any unmeasured total photonuclear cross sections. Moreover, the possibility of predicting cross section for partial photoreactions can be of use in planning future experiments.

It is hoped that the data discussed in this paper, together with their phenomenological interpretation, may be helpfull for a better understanding of the nuclear photoabsorption process.

Acknowledgments

One of us (OAPT) wishes to express his thanks to the Dipartimento di Scienze e Tecnologie Chimiche, Universita' degli Studi di Roma "Tor Vergata", for the warmest hospitality received during preparation of the manuscript. Partial support by the Italian INFN (Sezione di Roma 2) and by the Brazilian CNPq is also gratefully acknowledged.

FIGURE CAPTIONS

Fig. 1. Total nuclear photoabsorption cross section averaged over the 0.2-1.0 GeV interval, $\bar{\sigma}^{T}_{\gamma A}$, plotted against mass number A (upper line, (6)). The lower curve shows the contribution from the quasi-deuteron mechanism of primary photointeraction (second term in (5)).

Fig. 2. Total nuclear photoabsorption cross section per nucleon, $\sigma^{T}_{\gamma A}/A$, plotted against mass number A for different photon energy-values. The curves have been obtained from (2).

Fig. 3. Average total nuclear photoabsorption cross section per nucleon, $\langle\sigma^{T}_{\gamma A}/A\rangle$, plotted against photon energy. The upper full line with hatched area is the one obtained directly from the photomeson and quasi-deuteron primary photointeractions (8,9). The lower full line is the trend obtained without the quasi-deuteron contribution. The dashed line (taken from [76,77]) represents a smooth average of experimental data for nuclei $7 \leq A \leq 238$ (the "Universal Curve").

Fig. 4. Mean cross section for total pion photoproduction in the 0.2-1.0 GeV range, $\bar{\sigma}_t(\gamma,\pi)$, as a function of mass number A. Points represent calculated results as described in the text (Section 3.4).The straight line is the least-squares fit described in (18).

Fig. 5. Mean total photospallation cross section (0.2-1.0 GeV), $\bar{\sigma}_t(\gamma, sp)$, plotted against mass number A. The curve has been obtained from (20-23) and (25-27).

Fig. 6. Absolute mean photofission cross section in the energy range 0.2-1.0 GeV, $\bar{\sigma}(\gamma,F)$, as a function of parameter Z^2/A of the target nucleus. Data points are those listed in Table 2 (7th column), and the curve is an eye fit to the points. Values of $\bar{\sigma}(\gamma, F)$ for ^{nat}La [59], ^{154}Sm [43], ^{nat}Dy [64], and ^{174}Yb [43] have not been plotted.

Fig. 7. Total nuclear photoabsorption cross section averaged over the 0.2-1.0 GeV region, $\bar{\sigma}^{T}_{\gamma A}$, as a function of mass number A. Points represent $\bar{\sigma}^{T}_{\gamma A}$-values as obtained by summing the contributions from the various partial photoreactions (see text). The full straight line is a least-squares fit to the data points according to (29), and the hatched area represents the related uncertainty. The dashed line has been deduced from the primary photointeraction mechanisms (see (6)).

Fig. 8. The behaviour of the partial photonuclear reactions along

the Periodic Table. The figure shows the trend of the mean cross sections as a function of A for the indicated photoinduced processes in the energy range 0.2-1.0 GeV. The dashed portion of the (γ, sp)-curve has been obtained as described in the text (30).

Fig. 9a-b.Total photonuclear absorption cross section per nucleon, $\sigma^{T}_{\gamma A}/A$, plotted as a function of photon energy k for ^{4}He a and ^{6}Li b. The full lines have been calculated from (7). Experimental points in a have been taken from [18] ; in b from [14].

Fig.10a-b. The same as in Fig.9 for ^{7}Li a and ^{9}Be b. Experimental points in a have been taken from [14] ; in b from: [13] (Δ), [10] ($\square$), [18] ($\bigcirc$), [9] ($\blacktriangledown$), and [4] ($\bullet$).

Fig.11a-b.The same as in Fig.9 for ^{12}C a and ^{16}O b. Experimental points in a are from: [24] (Δ), [7] ($\bigcirc$), [10] ($\square$), [4] ($\bullet$), and [9] ($\blacktriangledown$); in b from: [18] ($\bigcirc$), and [9] (Δ).

Fig.12a-b. The same as in Fig.9 for ^{27}Al a and Ti b. Experimental points in a have been taken from: [7] (Δ), [18] ($\bigcirc$), and [9] ($\square$); in b from [18].

Fig.13a-b.The same as in Fig.9 for Ni a and Cu b. Experimental points in a have been taken from [7] ; in b from: [18] ($\bigcirc$), and [8] ($\square$).

Fig.14a-b.The same as in Fig.9 for Mo a and Sn b. Experimental points in a have been taken from [7] ; in b from [18].

Fig.15. The same as in Fig.9 for Pb. Experimental points have been taken from: [24] ($\square$), [21] ($\bigcirc$), [18] ($\bullet$), and [17] ($\blacktriangledown$).

Fig.16a-b. The same as in Fig.9 for ^{235}U a and ^{238}U b. Experimental points in a have been taken from: [19] ($\bigcirc$), [16] ($\bullet$), and [11] ($\square$); in b from : [1] (Δ), [19] ($\bigcirc$), [45] ($\square$), [16] ($\bullet$), [6] ($\blacksquare$), [4] ($\blacktriangle$), and [51] (dashed line).

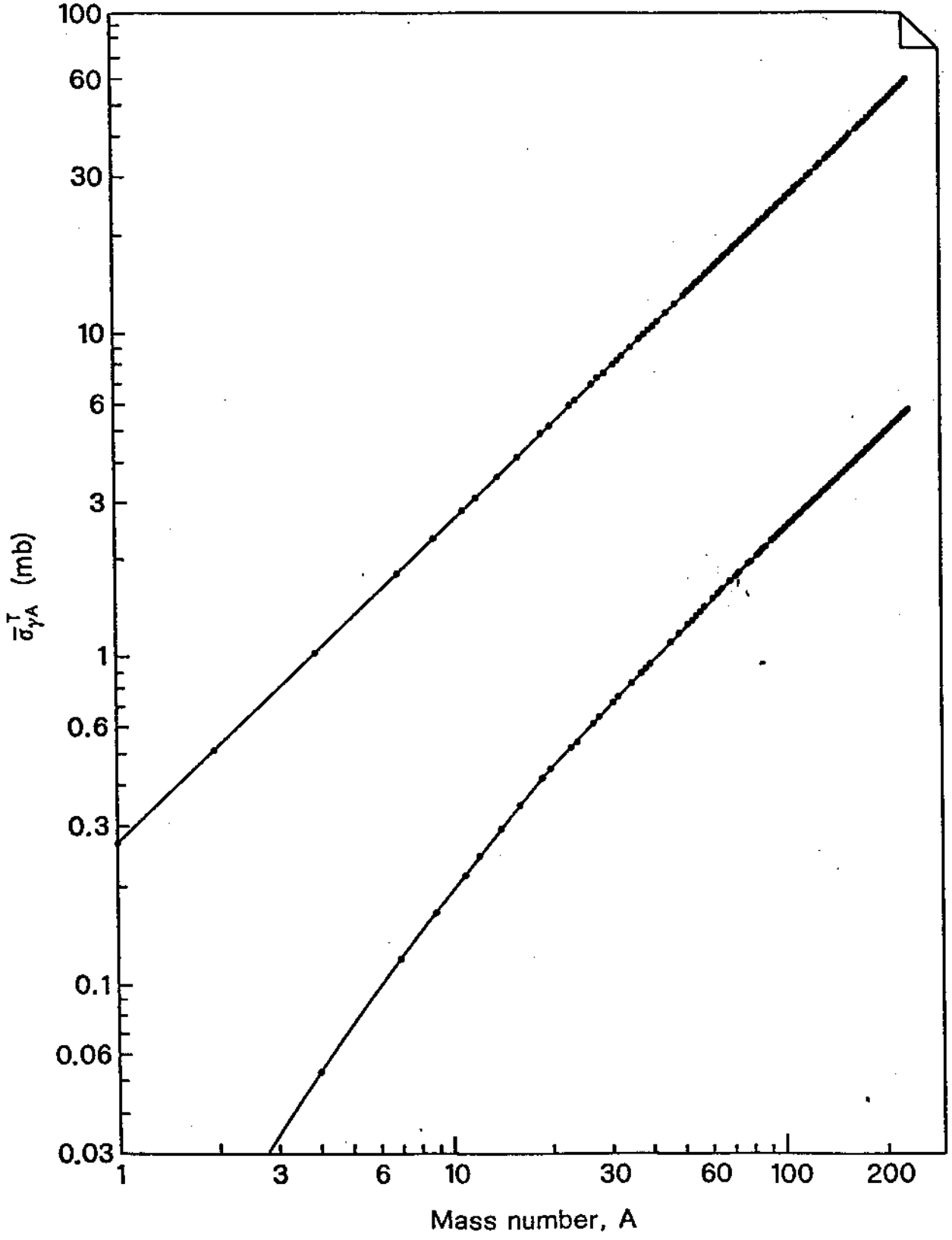
100
60
30
10
6
3
1
0.6
0.3
0.1
0.06
0.03
$\bar{\sigma}^{T}_{\gamma A}$ (mb)
1
3
6
10
30
60
100
200
Mass number, A

Fig. 1

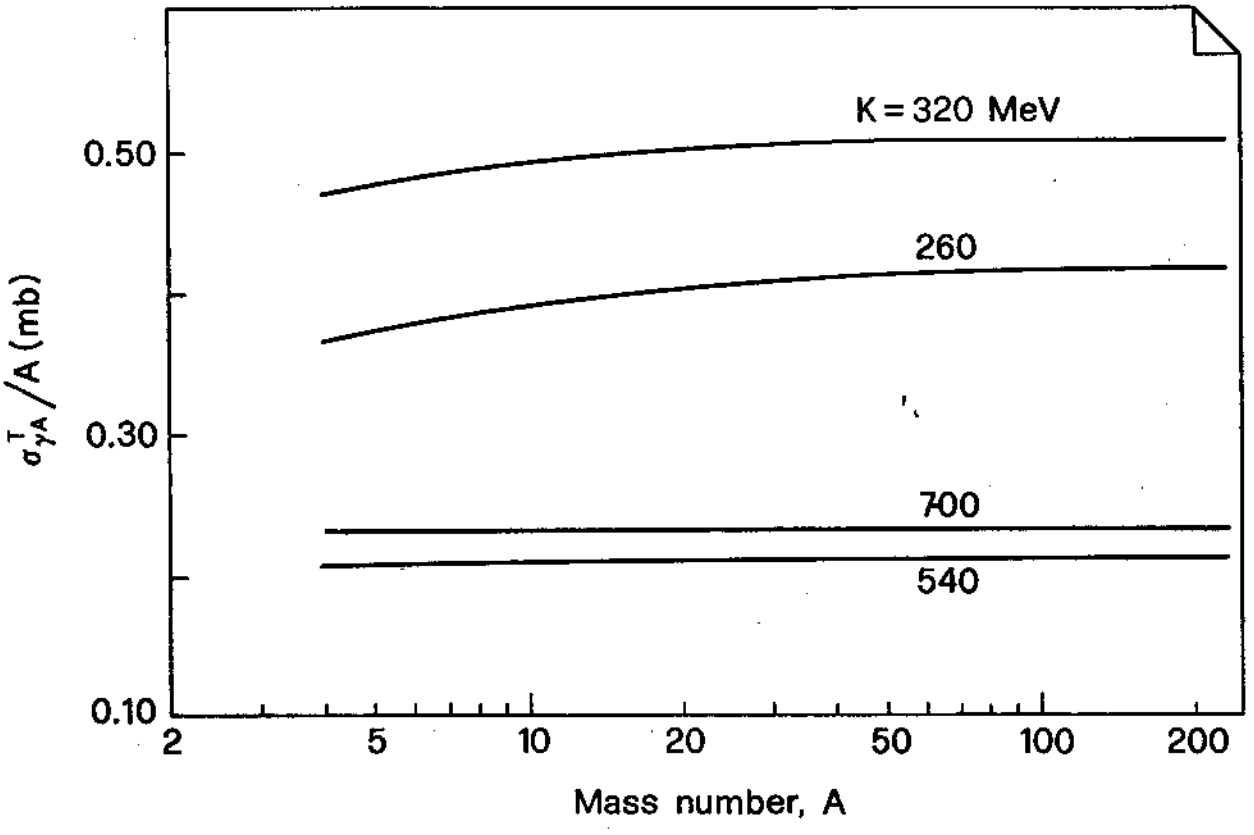
K = 320 MeV
260
700
540
0.50
0.30
0.10
$\sigma^T_{\gamma A}/A$ (mb)
2
5
10
20
50
100
200
Mass number, A

Fig. 2

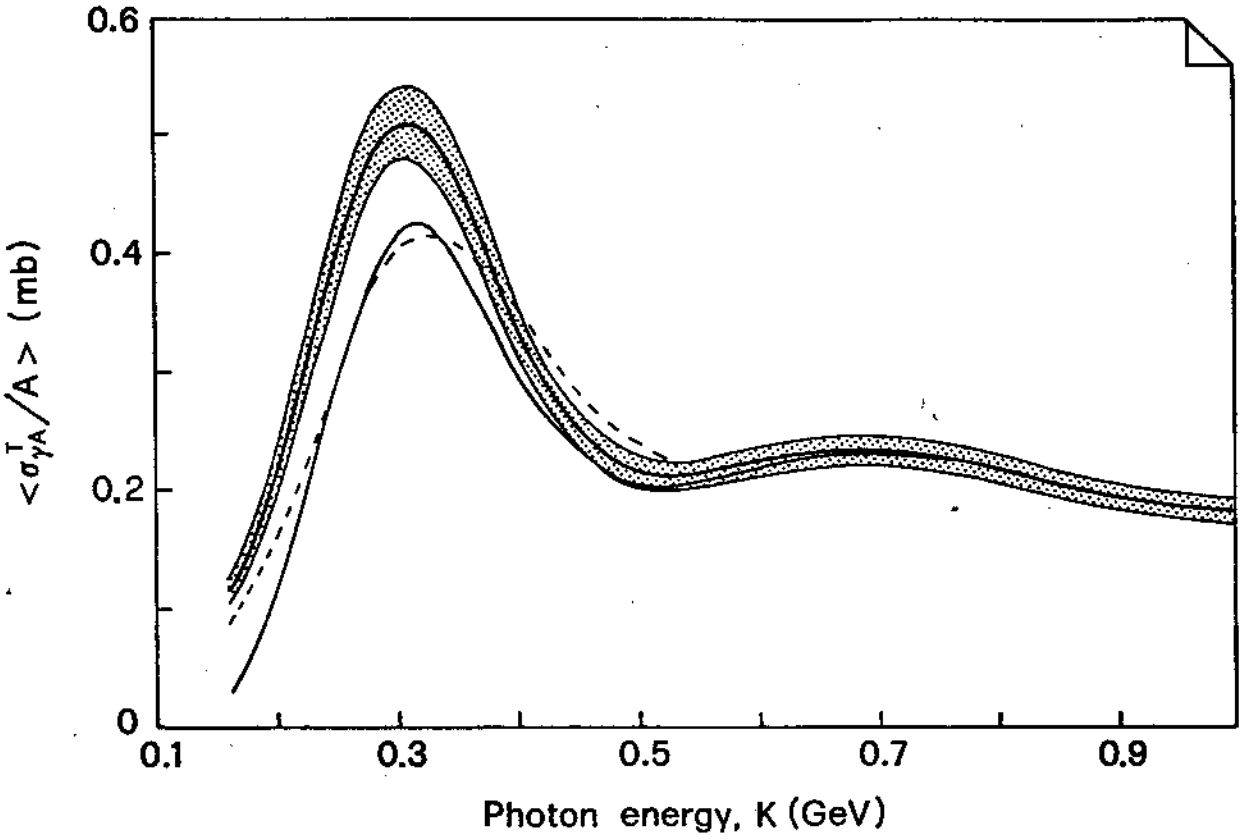

Fig. 3

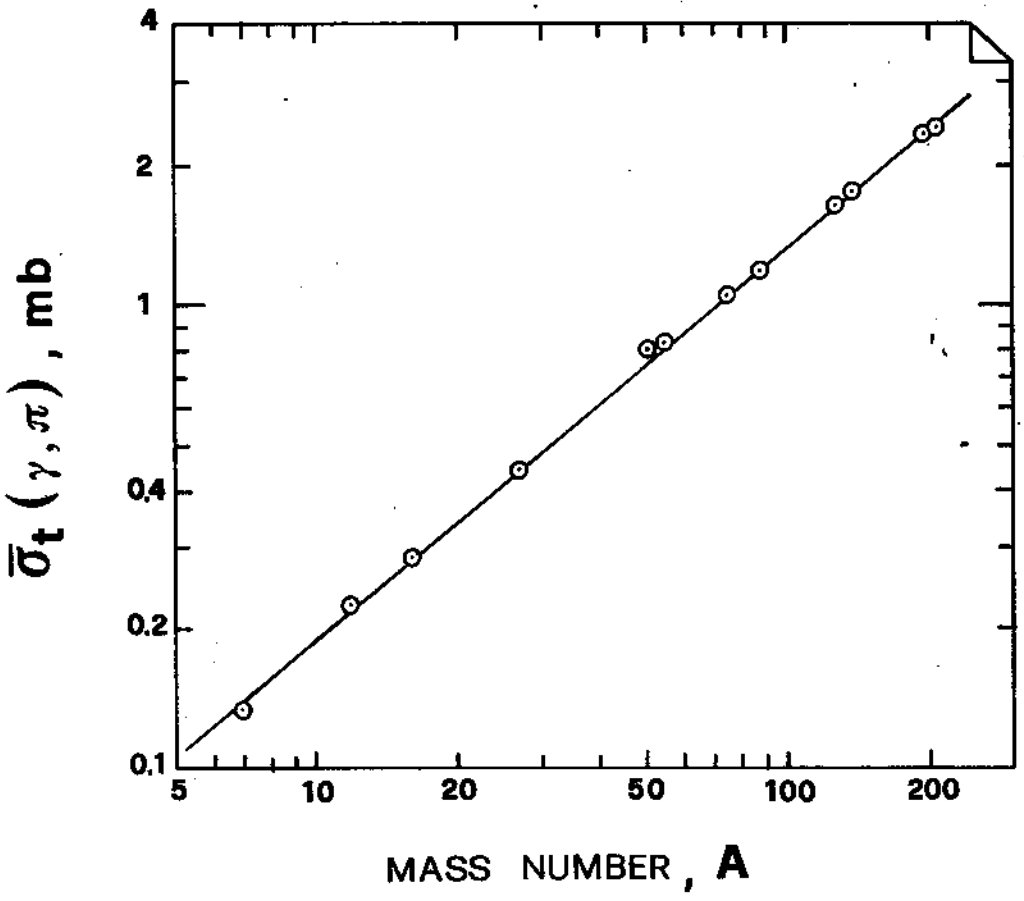
4
2
1
0.4
0.2
0.1
5
10
20
50
100
200
$\bar{\sigma}_t(\gamma,\pi)$, mb
MASS NUMBER, A

Fig. 4

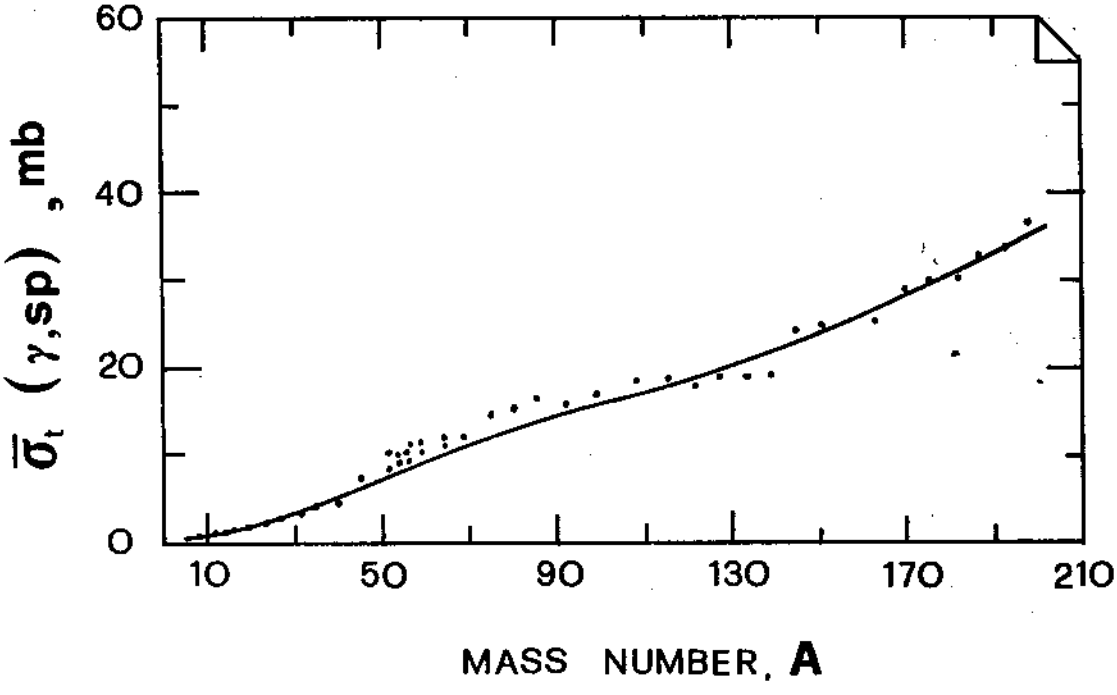
60
40
20
0
10
50
90
130
170
210
$\bar{\sigma}_t$ (γ,sp) , mb
MASS NUMBER, A

Fig. 5

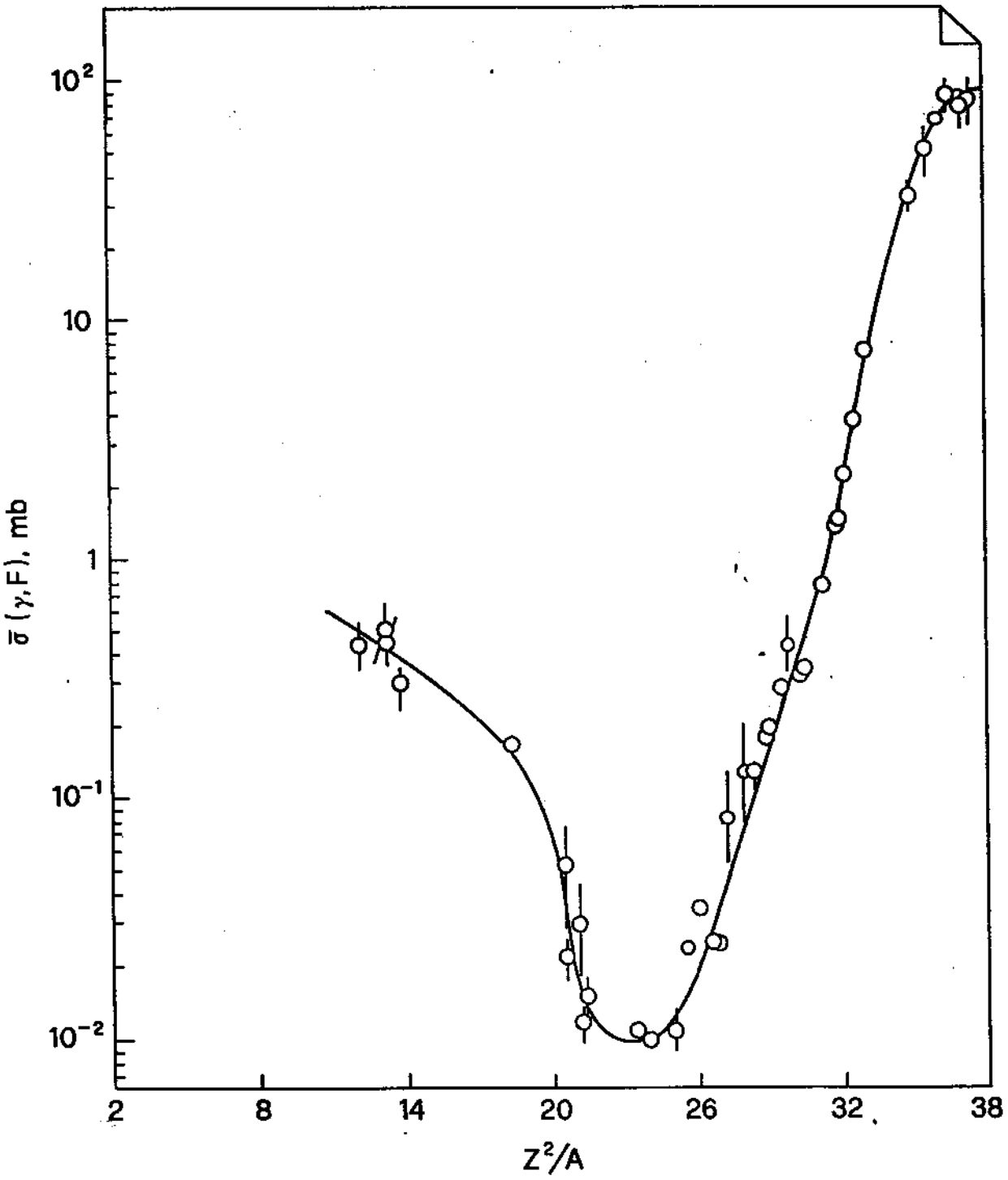

Fig. 6

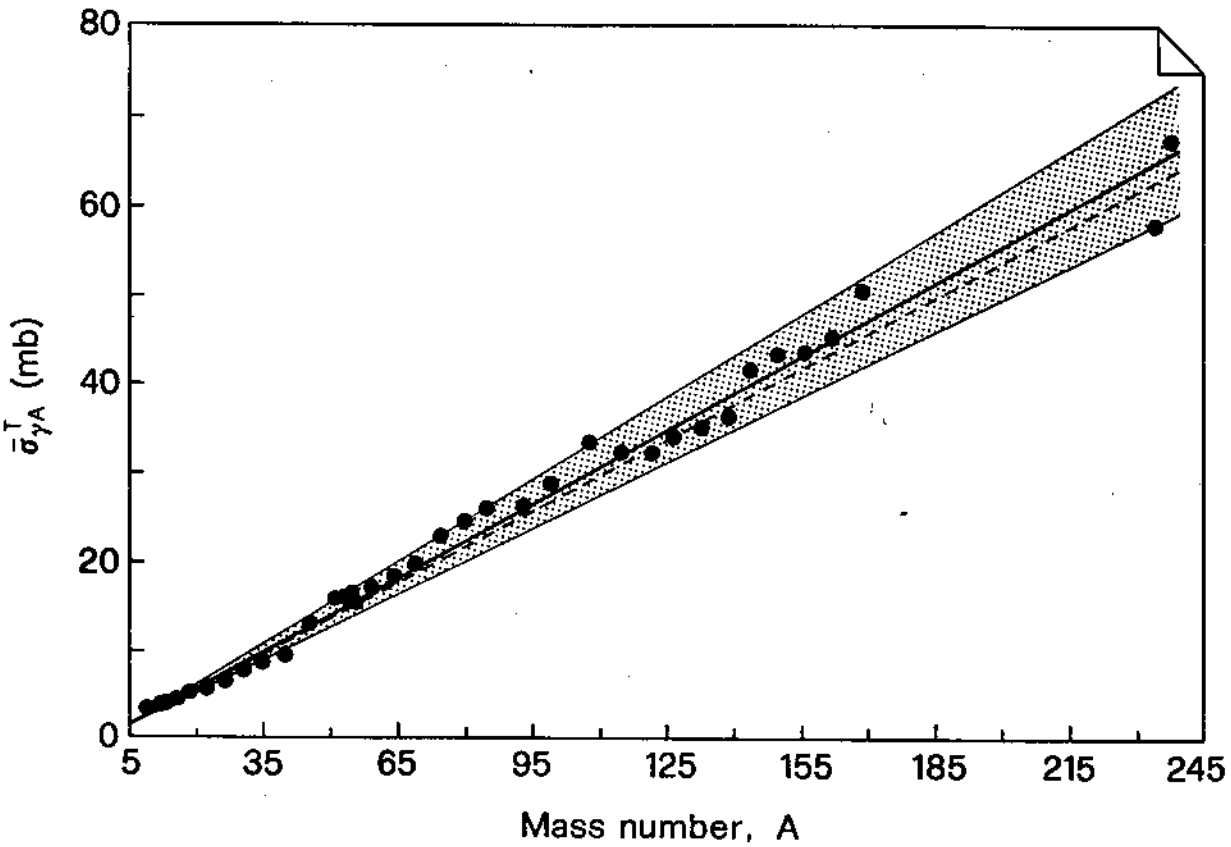
80
60
40
20
0
5
35
65
95
125
155
185
215
245
$\bar{\sigma}^{T}_{\gamma A}$ (mb)
Mass number, A

Fig. 7

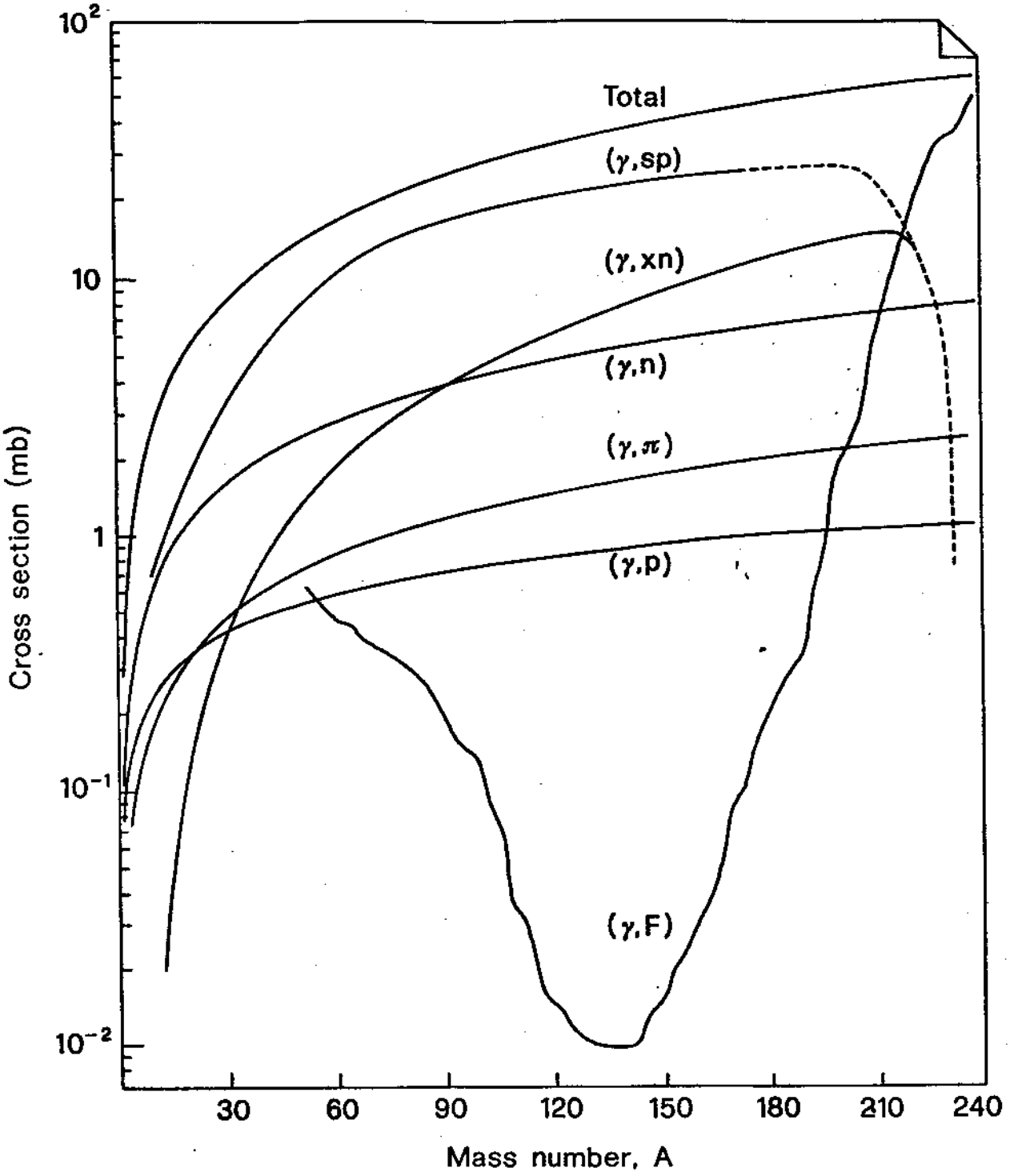
Total
(γ,sp)
(γ,xn)
(γ,n)
(γ,π)
(γ,p)
(γ,F)
Cross section (mb)
10²
10
1
10⁻¹
10⁻²
30
60
90
120
150
180
210
240
Mass number, A

Fig. 8

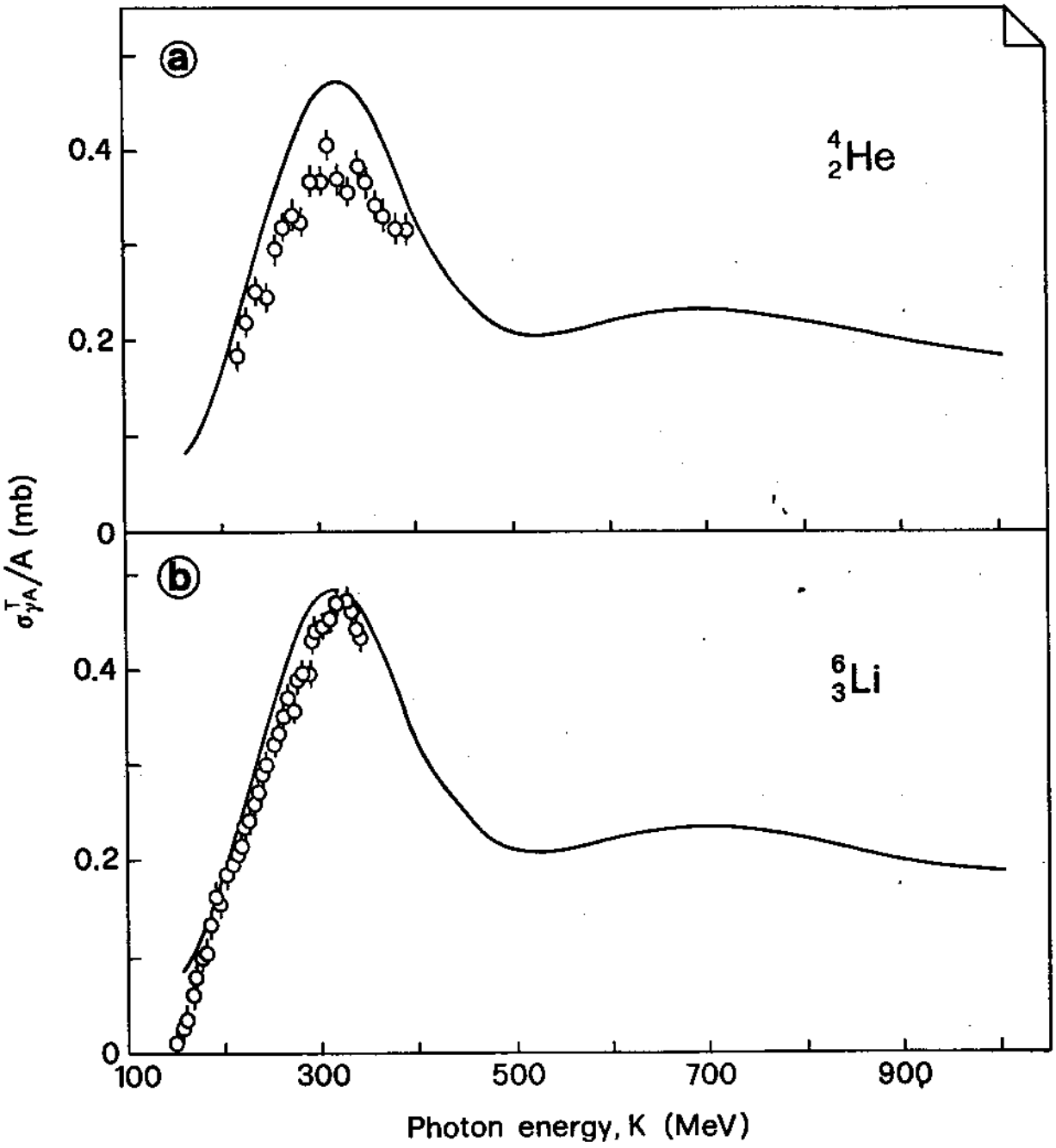
a
b
$^4_2$He
$^6_3$Li
0.4
0.2
0
100
300
500
700
900
$\sigma^T_{\gamma A}/A$ (mb)
Photon energy, K (MeV)

Fig. 9

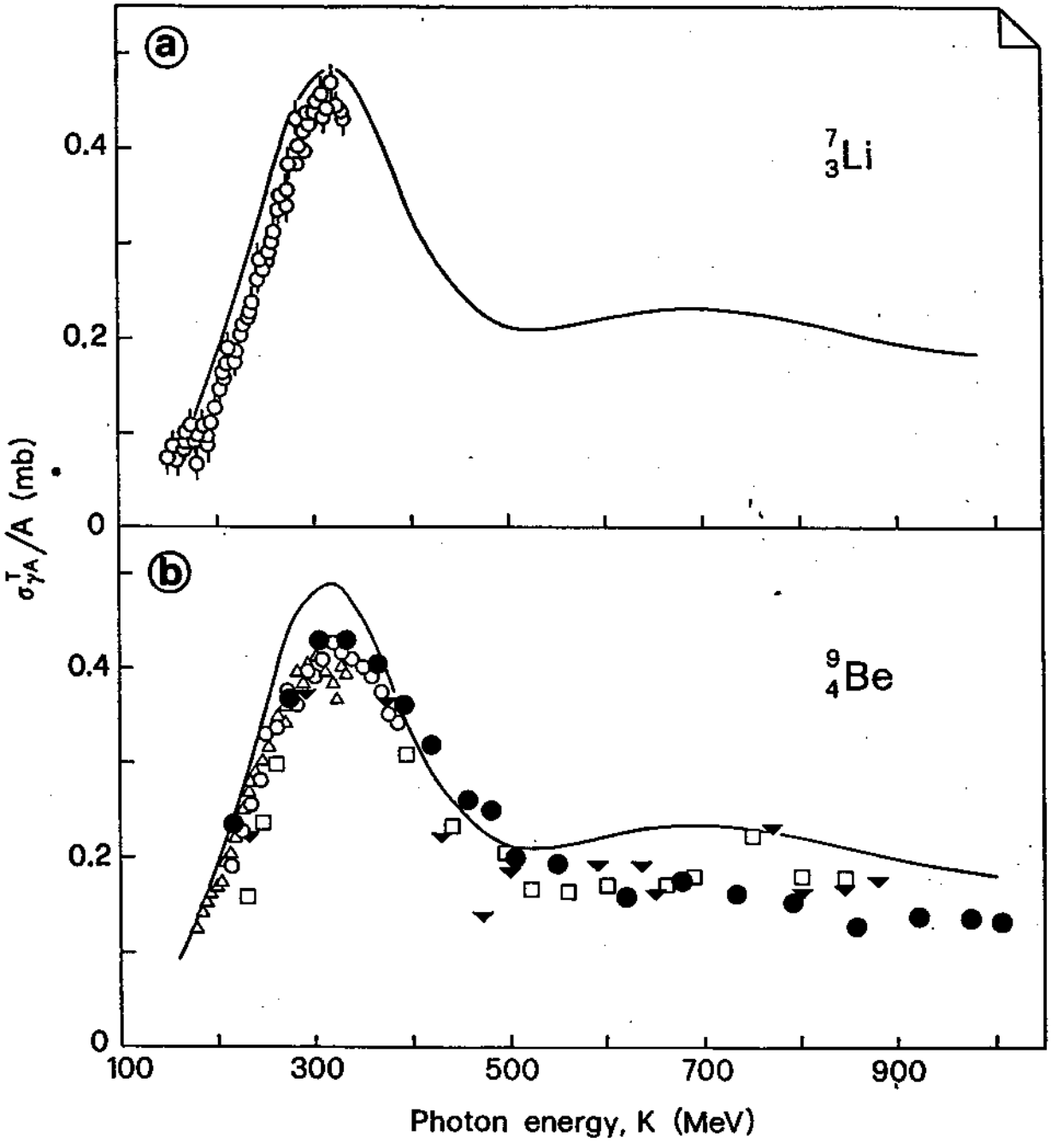
a
b
$^{7}_{3}$Li
$^{9}_{4}$Be
$\sigma^{T}_{\gamma A}/A$ (mb)
0
0.2
0.4
100
300
500
700
900
Photon energy, K (MeV)

Fig. 10

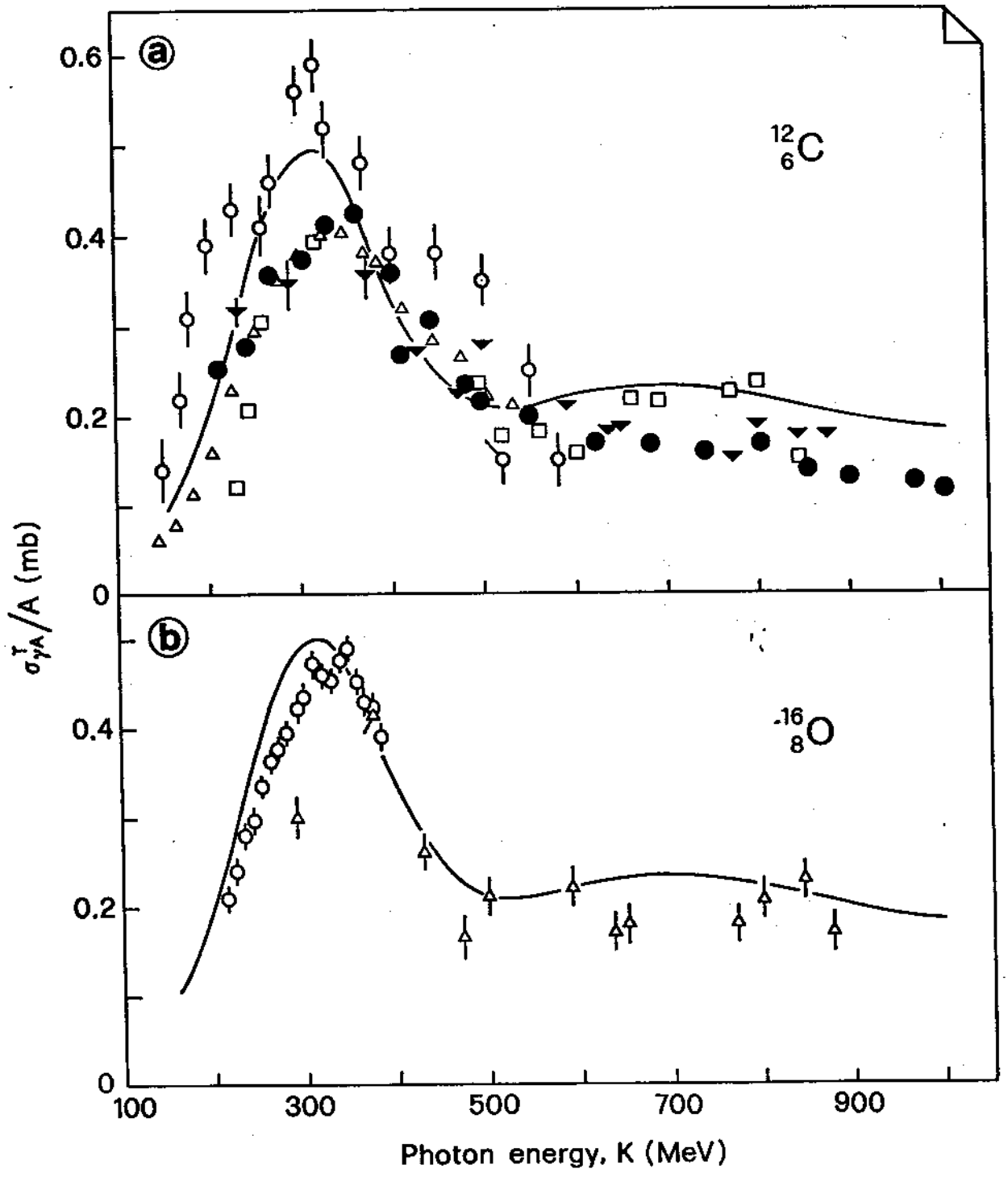
a
$^{12}_{6}C$
b
$^{16}_{8}O$
$\sigma^{\Gamma}_{\gamma A}/A$ (mb)
0.6
0.4
0.2
0
100
300
500
700
900
Photon energy, K (MeV)

Fig. 11

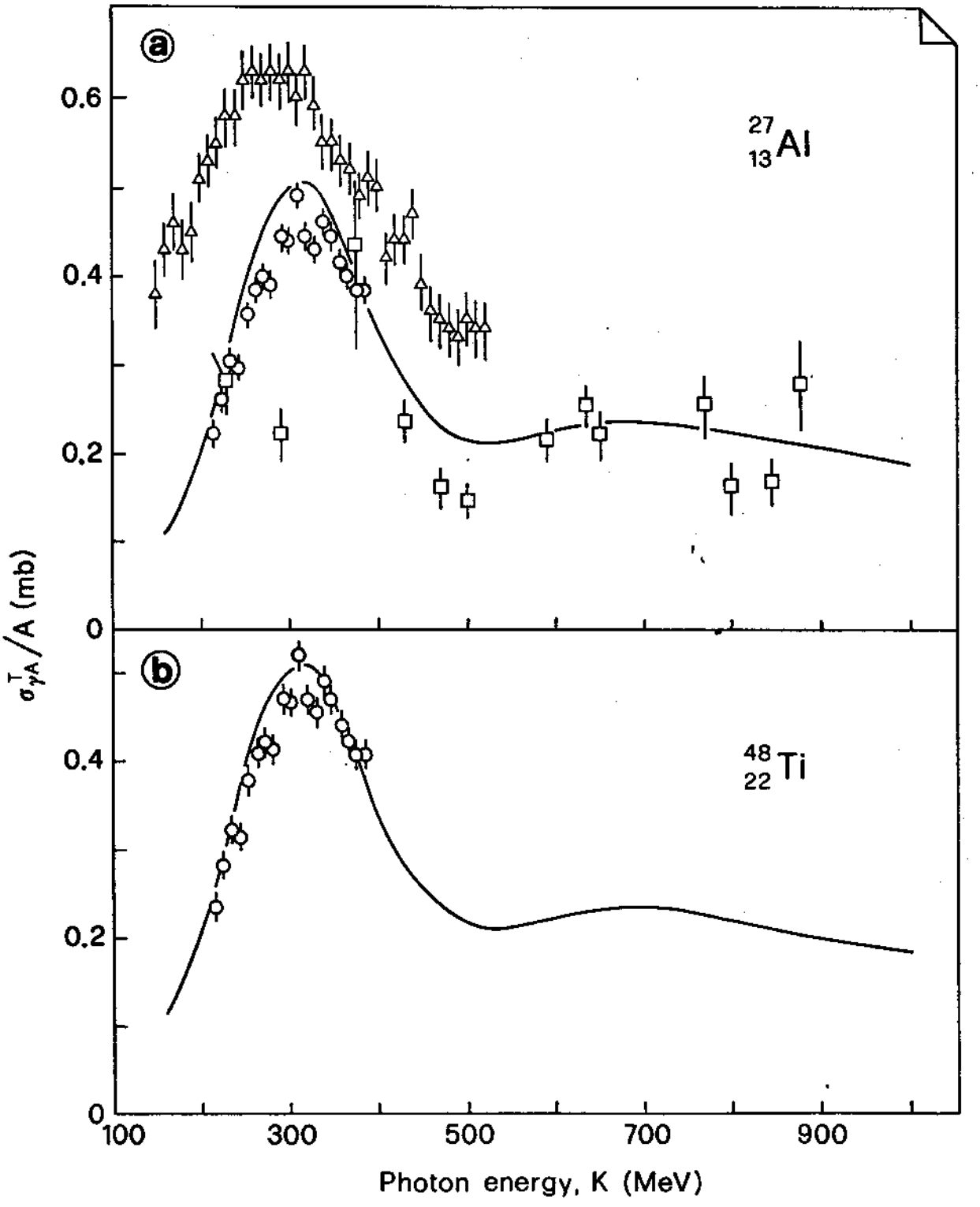
a
b
$^{27}_{13}$Al
$^{48}_{22}$Ti
$\sigma^{T}_{\gamma A}/A$ (mb)
0
0.2
0.4
0.6
100
300
500
700
900
Photon energy, K (MeV)

Fig. 12

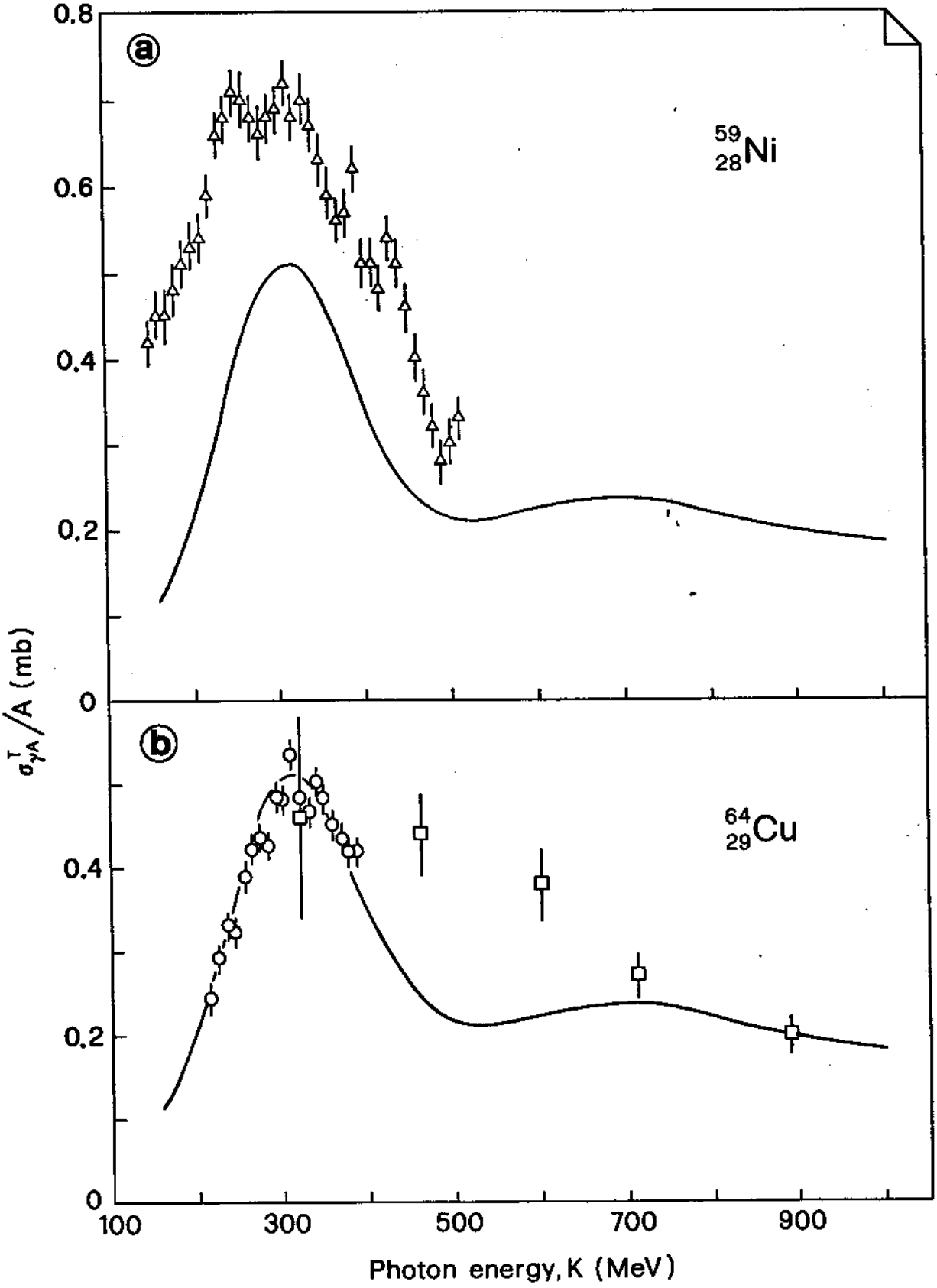
a
$^{59}_{28}$Ni
b
$^{64}_{29}$Cu
$\sigma^{I}_{\gamma A}/A$ (mb)
0.8
0.6
0.4
0.2
0
0.4
0.2
0
100
300
500
700
900
Photon energy, K (MeV)

Fig. 13

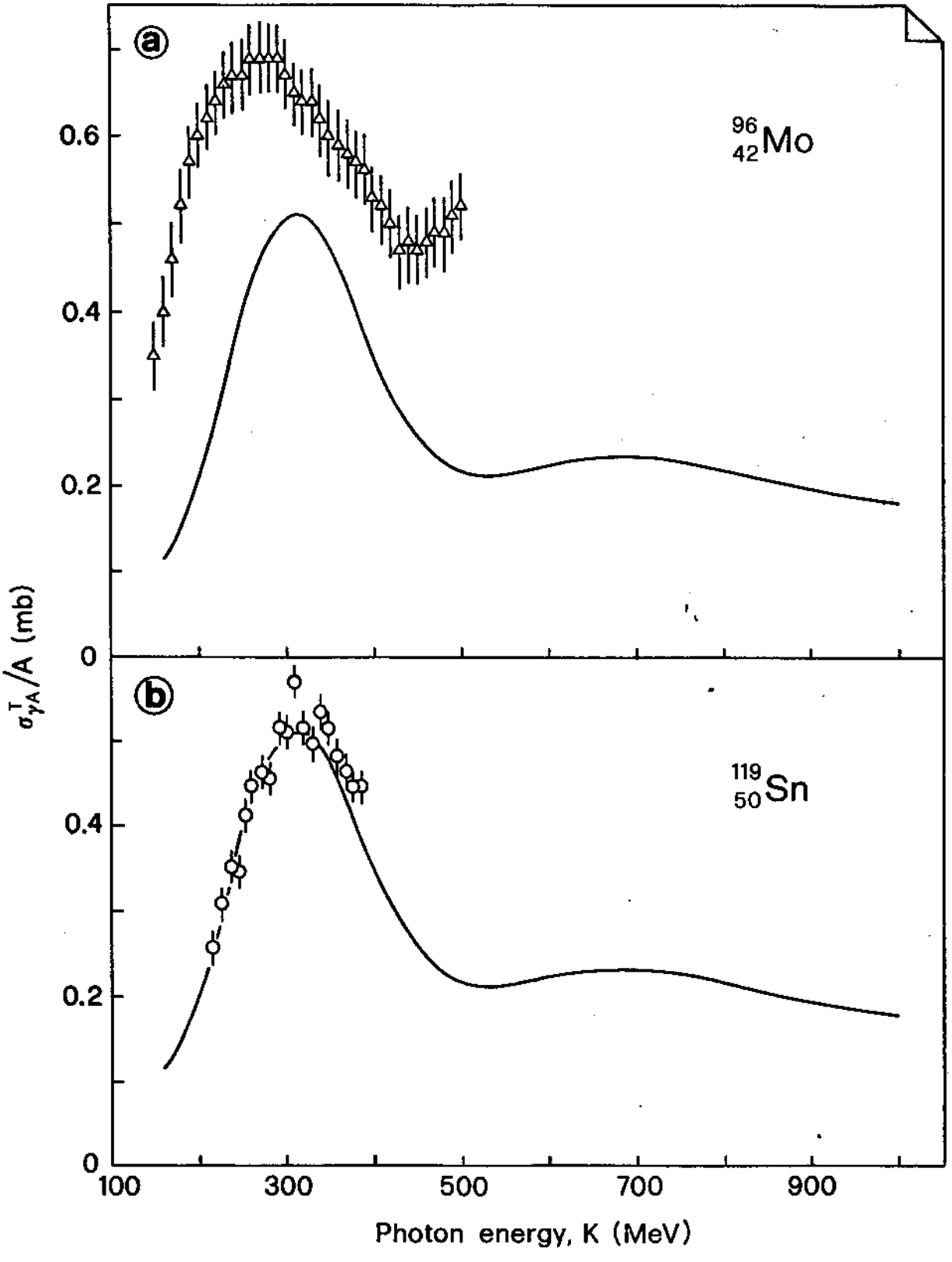
a
$^{96}_{42}$Mo
b
$^{119}_{50}$Sn
$\sigma^{T}_{\gamma A}/A$ (mb)
0
0.2
0.4
0.6
100
300
500
700
900
Photon energy, K (MeV)

Fig. 14

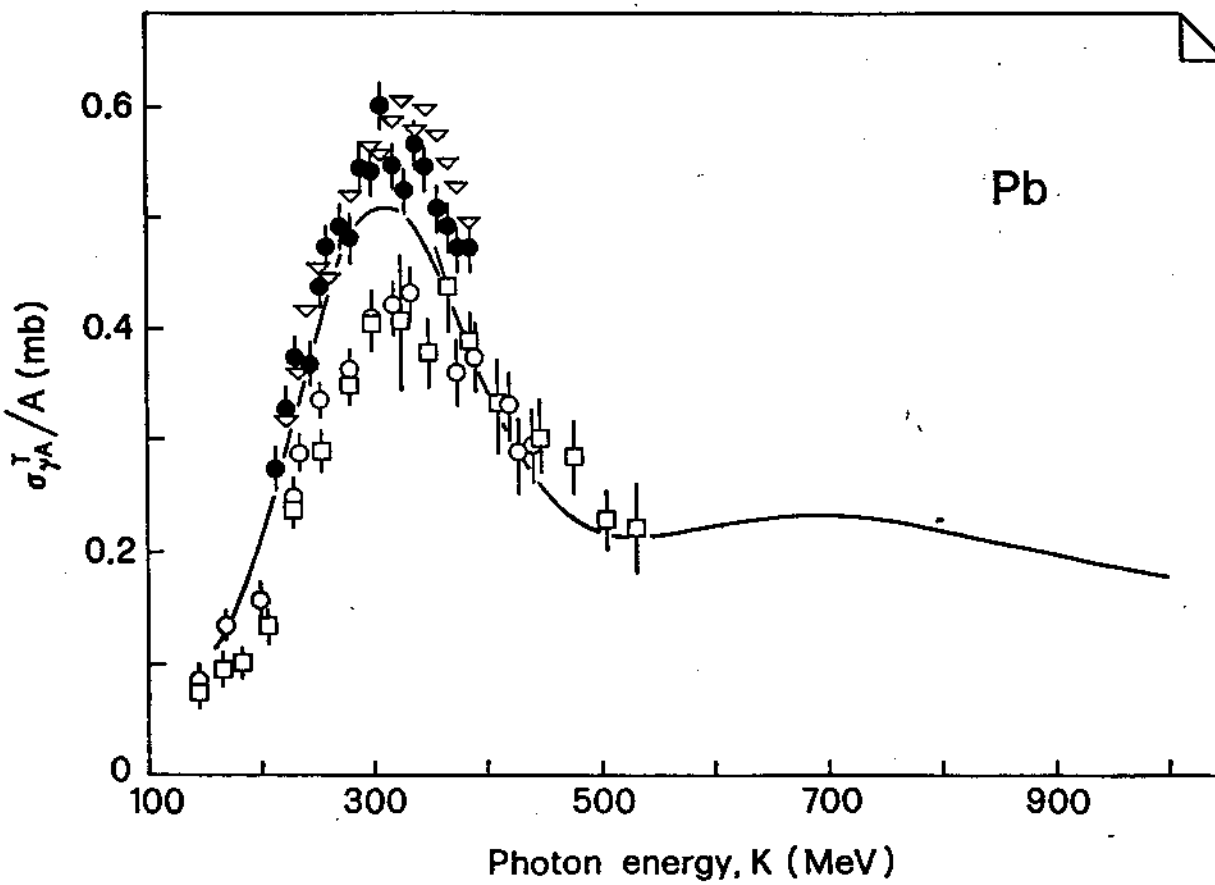
Pb
0.6
0.4
0.2
0
100
300
500
700
900
$\sigma^{I}_{\gamma A}/A$ (mb)
Photon energy, K (MeV)

Fig. 15

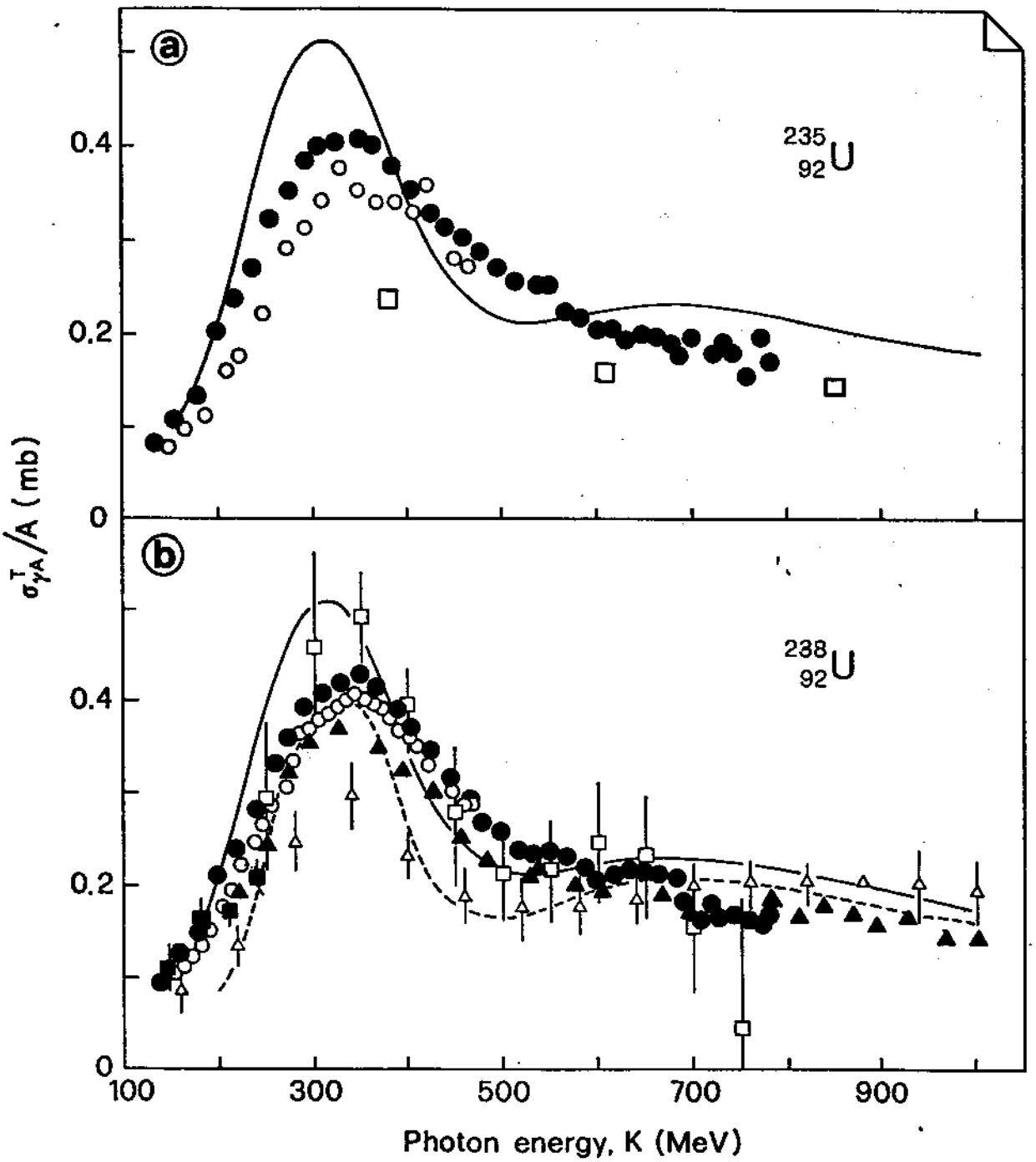
a
b
$^{235}_{92}U$
$^{238}_{92}U$
$\sigma^{T}_{\gamma A}/A$ (mb)
0
0.2
0.4
100
300
500
700
900
Photon energy, K (MeV)

Fig. 16

Table 1: Listing the experimental works on total nuclear photoabsorption cross section above the giant resonance ($E_\gamma > 20$ MeV)

Laboratory	Photon-source	Energy range (MeV)	Nuclei investigated	Ref.
Frascati	Coherent bremsstrahlung	160-1000	^{238}U	1
		200-500	^{238}U	2
	Positron annihilation	120-280	^{238}U	3
	Tagged photons	200-1200	Be, C, ^{238}U	4
Novosibirsk	Compton back-scattered photons	150-710	^{238}U, ^{237}Np	5
		60-240	^{238}U, ^{237}Np	6
Khar'kov	Virtual photons	150-500	C, Al, Ni, Mo, W	7
Yerevan	Tagged photons	250-2700	Be, C, O, Cu	8
		230-880	Be, C, O, Al	9
		230-850	Be, C	10
		310-3450	^{235}U, ^{238}U	11
Mainz	Bremsstrahlung	10-160	Li, Be, C, O, Al, Si, Ca	12
		150-340	^{6}Li, ^{7}Li, Be	13, 14
		178-330	Be	15
	Tagged photons	50-800	^{3}He, ^{235}U, ^{238}U	16
Bonn	Tagged photons	215-386	Pb	17
		215-386	He, Be, C, O, Al, Ti, Cu, Sn, Pb	18
		120-460	^{235}U, ^{238}U	19
Saclay	Positron annihilation	25-140	Sn, Ce, Ta, Pb, U	20
		145-440	Pb	21
		235, 330	Al, Cu, Zn, Sn, Ho, Ta, U	22
		145-440	Pb	22
	Tagged photons	40-105	^{235}U, ^{238}U	23
		130-530	C, Pb	24
		20-110	Th, ^{235}U, ^{238}U	25
Glasgow-Mainz	Bremsstrahlung	60-340	^{197}Au	26

Table 2. Compilation of absolute mean photofission cross section in the range ~ 0.2 - 1.0 GeV.

Element	Z	A	Z^2/A	Energy range (GeV)	$\bar{\sigma}$ (γ, F) (mb)	Average value	Ref.
Am	95	241	37.45	0.1-1.0	66[a]		63
						86±20	
				0.1-1.1	106		60
		243	37.14	0.1-1.0	76[a]		63
						87±10	
				0.1-1.1	98		60
Pu	94	239	36.97	0.1-1.0	80[a]	80±16	63
Np	93	237	36.49	0.1-1.0	77[a]		63
						90±12	
				0.15-0.71	102		5
U	92	235	36.02	0.1-1.0	76[a]		63
				0.2-1.0	69	69±6	51
				0.2-0.78	61		16
		238	35.56	0.1-1.0	45		1
				0.25-0.75	68		45
				0.15-1.0	57		43
				0.2-0.85	38		44
				0.2-1.0	41		51
				0.3-1.0	67	55±11	37
				0.3-1.0	43		52
				0.15-0.71	63		5
				0.3-1.0	60		35
				0.2-0.78	65		16
				0.22-1.0	54		4
Th	90	232	34.91	0.25-0.8	30		45
				0.2-0.85	29		44
				0.2-1.0	38	34±4	51
				0.3-1.0	37		37
				0.3-1.0	36		35
Bi	83	209	32.96	0.3-1.0	6.5		35
				0.3-1.0	7.8		36
				0.2-1.0	7.6		59
						7.5±0.5	
				0.3-1.0	7.6		47
					7.8		41
				0.2-1.0	3.7		43
Pb	82	207.2	32.45	0.3-0.9	5		48
				0.22-1.0	3.6		59
				0.3-1.0	3.3		47
						3.9±0.6	
				0.25-1.0	4		53
					3.4		41
				0.2-1.0	3.9		43
Tl	81	204.4	32.10	0.23-1.0	2.8		59
				0.3-1.0	1.9	2.3±0.4	46
					2.1		41
Hg	80	200.6	31.90	0.3-1.0	1.5	1.5±0.1	46
Au	79	197	31.68	0.3-0.9	1.7		48
				0.24-1.0	1.4		59
				0.3-1.0	1.36		52
						1.4±0.2	
				0.3-1.0	1.19		46
				0.25-1.0	1.5		53
					1.25		41

Pt	78	195.1	31.18	0.26-1.0	0.80		59
						0.80±0.07	
					0.80		41
Os	76	190.3	30.35	0.3-1.0	0.35	0.35±0.05	41
Re	75	186.2	30.21	0.28-1.0	0.29		59
						0.32±0.03	
					0.34		41
W	74	183.9	29.78	0.3-1.0	0.65		36
						0.47±0.20	
				0.29-1.0	0.28		59
Ta	73	181	29.44	0.3-0.9	0.33		48
				0.3-1.0	0.27	0.29±0.03	59
					0.27		41
Hf	72	178.5	29.04	0.31-1.0	0.14		59
						0.20±0.06	
					0.25		41
Lu	71	175	28.81		0.18	0.18±0.04	64
Yb	70	173	28.32	0.3-0.9	0.12		48
				0.33-1.0	0.12	0.13±0.02	59
					0.16		64
		174	28.16	0.2-1.0	0.37	0.37±0.07	43
Tm	69	169	28.17	0.34-1.0	6.8×10^{-2}		59
						0.13±0.07	
					0.20		64
Ho	67	165	27.21	0.3-0.9	5.5×10^{-2}		48
				0.36-1.0	3.5×10^{-2}	$(8\pm5)\times10^{-2}$	59
					0.15		64
Dy	66	162.5	26.81	0.36-1.0	2.5×10^{-2}		59
						2.5×10^{-2}	
					(0.21)		64
Tb	65	159	26.57	0.37-1.0	2.5×10^{-2}	2.5×10^{-2}	59
Gd	64	157.3	26.04	0.3-0.9	5.3×10^{-2}		48
						3.5×10^{-2}	
				0.38-1.0	1.7×10^{-2}		59
Sm	62	150.4	25.56	0.39-1.0	1.4×10^{-2}		59
						2.5×10^{-2}	
					2.9×10^{-2}		64
		154	24.96	0.25-1.05	6.1×10^{-2}	$(6.1\pm1.2)\times10^{-2}$	43
Nd	60	144.3	24.95	0.3-0.9	1.3×10^{-2}		48
				0.41-1.0	1.0×10^{-2}	$(1.1\pm0.2)\times10^{-2}$	59
					9×10^{-3}		64
Ce	58	140.2	23.99	0.42-1.0	$(9\pm1)\times10^{-3}$		59
La	57	139	23.37	0.3-0.9	1.1×10^{-2}		48
						1.1×10^{-2}	
				0.43-1.0	(1.0×10^{-3})		59
Sb	51	121.8	21.35	0.46-1.0	1.5×10^{-2}	$(1.5\pm0.3)\times10^{-2}$	59
Te	52	127.6	21.19	0.47-1.0	1.2×10^{-2}	$(1.2\pm0.2)\times10^{-2}$	59
Sn	50	118.7	21.06	0.3-0.9	4.3×10^{-2}		48
						$(3.0\pm1.3)\times10^{-2}$	
				0.47-1.0	1.7×10^{-2}		59
Cd	48	112.5	20.48	0.47-1.0	2.2×10^{-2}	$(2.2\pm0.4)\times10^{-2}$	59
Ag	47	108	20.45	0.3-0.9	8.4×10^{-2}		48
				0.47-1.0	2.6×10^{-2}	$(5.3\pm2.4)\times10^{-2}$	59
				0.3-1.0	5×10^{-2}		36
Mo	42	96	18.38	0.3-0.9	0.17	0.17±0.04	48
Zn	30	65.4	13.76	0.52-1.0	0.3	0.30±0.06	59
Cu	29	63.6	13.22	0.3-0.9	0.66		48
						0.51±0.15	
				0.52-1.0	0.36		59
Ni	28	58.8	13.33	0.3-0.9	0.58		48
						0.47±0.11	
				0.51-1.0	0.36		59
Fe	26	55.9	12.09	0.51-1.0	0.44	0.44±0.09	59

[a] Assuming 55 ± 11 mb for ^{238}U.

REFERENCES

[1] Bellini, V., Emma, V., Lo Nigro, S., Milone, C., Pappalardo, G.S., Bologna, G.: Nuovo Cimento A55, 182 (1980)

[2] Bellini, V., Emma, V., Lo Nigro, S. Milone, C., Pappalardo, G.S., Santagati, M., Bologna, G.: Nuovo Cimento A71, 229 (1982)

[3] Bellini, V., Emma, V., Lo Nigro, S., Milone, C., Pappalardo, G.S., De Sanctis, E., Di Giacomo, P., Guaraldo, C., Lucherini, V., Polli, E., Reolon, A.R.: Nuovo Cimento, A85, 75 (1985)

[4] Bianchi, N., Deppman, A., De Sanctis, E., Fantoni, A., Levi Sandri, P., Lucherini, V., Muccifora, V., Polli, E., Reolon, A.R., Rossi, P., Anghinolfi, M., Corvisiero, P., Gervino, G., Mazzaschi, L., Mokeev, V., Ricco, G., Ripani, M., Sanzone, M., Taiuti, M., Zucchiatti, A., Bergère, R., Carlos, P., Garganne, P., Leprêtre, A.: Phys. Lett. B299, 219 (1993); see also: Anghinolfi, M., et al.: Nucl. Phys. A553, 631c (1993)

[5] Kazakov, A.A., Kezerashvili, G.Ya., Lazareva, L.E., Nedorezov, V.G., Skrinskii, A.N., Sudov, A.S., Tumaikin, G.M., Shatunov, Yu.M.: JETP Lett. 40, 1271 (1984)

[6] Iljinov, A.S. Ivanov, D.I., Mebel, M.V., Nedorezov, V.G., Sudov, A.S., Kezerashvili, G.Ya., Nucl. Phys. A539, 263 (1992)

[7] Vlasenko, V.G., Gol'dshtein, V.A., Mitrofanova, A.V., Noga, V.I., Ranyuk, Yu.N., Startsev, V.I., Sorokin, P.V., Telegin, Yu.N.: Sov. J. Nucl. Phys. 23, 265 (1976)

[8] Arakelyan, E.A., Bayatyan, G.L., Vartanyan, G.S., Grigoryan, N.K., Kechechyan, A.O., Knyazyan, S.G., Margaryan, A.T., Marikyan, G.G., Stepanyan, S.S., Shakhazizyan, S.R.: Sov. J. Nucl. Phys. 38, 589 (1983)

[9] Arakelyan, E.A., Bayatyan, G.L., Vartanyan, G.S., Voskanyan, A.R., Grigoryan, N.K., Knyazyan, S.G., Margaryan, A.T., Marikyan, G.G., Stepanyan, S.S., Oganesyan, E.M., Shakhazizyan, S.R.: Sov. J. Nucl. Phys. 42, 1 (1985)

[10] Ananikyan, A.K., Arakelyan, E.A., Bayatyan, G.L., Vartanyan, G.S., Voskanyan, A.R., Darbinyan, K.T., Grigoryan, N.K., Knyazyan, S.G., Margaryan, A.T., Marikyan, G.G., Mkrtchyan, K.K., Oganesyan, E.M., Simonyan, S.G., Stepanyan, S.S., Shakhazizyan, S.R.: Sov. J. Nucl. Phys. 46, 208 (1987)

[11] Arakelyan, E.A., Bagdsaryan, A.R., Bayatyan, G.L, Vartanyan, G.S., Voskanyan, A.R., Grigoryan, N.K., Knyazyan, S.G., Margaryan, A.T., Marikyan, G.G., Papyan, A.K.: Sov. J. Nucl. Phys. 52, 878 (1990)

[12] Ahrens, J., Borchert, H., Czock, K.H., Eppler, H.B., Gimm, H., Gundrum, H., Kroning, M., Riehn, P., Sita Ram, G., Zieger, A., Ziegler, B.: Nucl. Phys. A251, 479 (1975)

[13] Ahrens, J., Gimm, H.A., Hughes, R.J., Leicht, R., Minn, P., Zieger, A., Ziegler, B.: In: Photopion Nuclear Physics. Stoler, P. (ed.), p. 385. N.York: Plenum 1979

[14] Ziegler, B.: In: Lecture Notes in Physics, vol. 108, p. 148. Berlin: Springer 1979

[15] Ahrens, J.: In : Proceedings of the International Conference on High Energy Physics and Nuclear Structure, Vancouver 1979. Measday, D.F., Thomas,A.W. (eds.), p. 67. Amsterdam: North-Holland 1980.

[16] Frommhold, Th., Steiper, F., Henkel, W., Kneissl, U., Ahrens, J., Beck, R., Peise, J., Schmitz, M.: Phys. Lett. B295, 28 (1992); see also: Institute fur Strahlenphysik, Universitat Stuttgart, Annual Report, pp. 33 (1992); Ahrens, J.: Nucl. Phys. A553, 625c (1993)

[17] Rost, H.: Dissertation, Bonn-IR-80-10, Bonn Universitat (1980)
[18] Arends, J., Eyink, J., Hegerath, A., Hilger, K.G., Mecking, B., Noldeke, G., Rost, H.: Phys. Lett. B98, 423 (1981)
[19] Ahrens, J., Arends, J., Bourgeois, P., Carlos, P., Fallou, J.L., Floss, N., Garganne, P., Huthmacher, S., Kneissl, U., Mank, G., Mecking, B., Ries, H., Stenz, R., Veyssière, A., Phys. Lett. B146, 303 (1984)
[20] Leprêtre, A., Beil, H., Bergère, R., Carlos, P., Fagot, J., De Miniac, A., Veyssière, A.: Nucl. Phys. A367, 237 (1981)
[21] Chollet, C., Arends, J., Beil, H., Bergère, R., Bourgeois, P., Carlos, P., Fallou, J.L., Fagot, J., Garganne, P., Leprêtre, A., Veyssière, A.: Phys. Lett. B127, 331 (1983)
[22] Carlos, P., Beil, H., Bergère, R., Fagot, R., Leprêtre, A., De Miniac, A., Veyssière, A.: Nucl. Phys. A431, 573 (1984)
[23] Ries, H., Kneissl, U., Mank, G., Stroher, H., Wilke, W., Bergère, R., Bourgeois, P., Carlos, P., Fallou, J.L., Garganne, P., Veyssière, A., Cardman, L.S.: Phys. Lett. B139, 254 (1984)
[24] Ghedira, M.L.: In: Proceedings of the 8-ème Session de Physique Nucleaire, Aussois 1985, S.9-1
[25] Leprêtre, A., Bergère, R., Bourgeois, P., Carlos, P., Fagot, J., Fallou, J.L., Garganne, P., Veyssière, A., Ries, H., Gobel, R., Kneissl, U., Mank, G., Stroher, H., Wilke, W., Ryckbosch, D., Jury, J.: Nucl.Phys. A472, 533 (1987)
[26] Anthony, I., Branford, D., Flowers, A.G., McGeorge, J.C., Sené, M.R., Shotter, A.C., Thorley, P.J., Zimmerman, C.H., Friedrich, J., Voegler, N., Bangert, K., Berg, U.E.P.: Phys. Lett. B141, 309 (1984)
[27] Carlos, P.: In: Proceedings of the Fifth Course of the International School of Intermediate Energy Nuclear Physics, Verona (Italy) 1985. Bergère, R., Costa, S., Schaerf, C., (eds.), p.1. Singapore: World Scientific 1986
[28] Levinger, J.S., Phys. Rev. 84, 43 (1951)
[29] Levinger, J.S., Phys. Lett. B82, 181 (1979)
[30] Bauer, T.H., Spital, R.D., Yennie, D.R., Pipkin, F.M.: Rev. Mod. Phys. 50, 261 (1978)
[31] Caldwell, D.O., Cumalat, J.P., Eisner, A.M., Lu, A., Morrison, R.J., Murphy, F.V., Yellin S.J., Davis, P.J., Donnelly, M.G., Egloff, R.M., Luste, G.J., Martin, J.F., Prentice, J.D., Nash, T.: Phys. Rev. Lett. 42, 553 (1979)
[32] Ahrens, J., Ferreira, L.S., Weise, W.: Nucl. Phys. A485, 621 (1988)
[33] Hughes, I.S., March, P.V.: Proc. Phys. Soc. (London) 72, 259 (1958)
[34] March, P.V., Walker, T.G.: Proc. Phys. Soc.(London) 77, 293 (1961)
[35] de Carvalho, H.G., Celano, A., Cortini, G., Rinzivillo, R., Ghigo, G.: Nuovo Cimento (serie X) 19, 187 (1961)
[36] de Carvalho, H.G., Cortini, G., Del Giudice, E., Potenza, G., Rinzivillo, R., Ghigo, G.: Nuovo Cimento (serie X) 32, 293 (1964)
[37] Carbonara, F., de Carvalho, H.G., Rinzivillo, R., Sassi, E., Murtas, G.P.: Nucl. Phys. 73, 385 (1965)
[38] Meyer, R.A., Walters, W.B., Hummel, J.P.: Phys. Rev.138, B1421 (1965)
[39] Meyer, R.A., Hummel, J.P.: Phys. Rev. 140 , B 48 (1965)
[40] Walters, W.B., Hummel, J.P.: Phys. Rev. 143, 833 (1966)
[41] Mitrofanova, A.V., Ranyuk, Yu.N., Sorokin, P.V.: Sov. J. Nucl. Phys. 6, 512 (1968)
[42] Nydahl, G., Forkman, B.: Nucl. Phys. B7, 97 (1968)
[43] Moretto, L.G., Gatti, R.C., Thompson, S.G., Routti, J.T., Heisenberg,

J.H., Middleman, L.M., Yearian, M.R., Hofstadter, R.: Phys. Rev. 179, 1176 (1969)
[44] Methasiri, T.: Nucl. Phys. A158, 433 (1970)
[45] Wakuta, Y.: J. Phys. Soc. Japan 31, 12 (1971)
[46] Emma, V., Lo Nigro, S., Milone, C.: Lett. Nuovo Cimento 2,271 (1971)
[47] Emma, V., Lo Nigro, S., Milone, C.: Lett. Nuovo Cimento 2, 117 (1971)
[48] Methasiri, T., Johansson, S.A.E.: Nucl. Phys. A167, 97 (1971)
[49] Blomqvist, I., Nydahl, G., Forkman, B.: Nucl. Phys. A162, 193 (1971).
[50] Andersson, G., Blomqvist, I., Forkman, B., Jonsson, G.G., Jarund, A., Kroon, I., Lindgren, K., Schroder, B.: Nucl. Phys. A197, 44 (1972)
[51] Vartapetyan, G.A., Demekhina, N.A., Kasilov, V.I., Ranyuk, Yu.N., Sorokin, P.V., Khudaverdyan, A.G.: Sov. J. Nucl. Phys. 14, 37 (1972)
[52] David, P., Debrus, J., Kim, U., Kumbartzki, G., Mommsen, H., Soyez, W., Speidel, K.H., Stein, G.: Nucl. Phys. A197, 163 (1972)
[53] Kroon, I., Forkman, B.: Nucl. Phys. A179, 141 (1972)
[54] Jonsson, G.G., Lindgren, K.: Phys. Scr. 7, 49 (1973) and references therein.
[55] di Napoli, V., Salvetti, F., Terranova, M.L., de Carvalho, H.G., Martins, J.B.: Phys. Rev. C8, 206 (1973)
[56] di Napoli, V., Salvetti, F., Terranova, M.L., de Carvalho, H.G., Martins, J.B., Tavares, O.A.P.: Gazz. Chim. Ital. 105, 317 (1975) and references therein.
[57] Bulow, B., Johnsson, B., Nillson, M., Forkman, B.: Z. Phys. A278, 89 (1976)
[58] di Napoli, V., Rosa, G., Salvetti, F., Terranova, M.L., de Carvalho, H.G., Martins, J.B., and Tavares, O.A.P.: J. Inorg. Nucl. Chem. 38, 1 (1976)
[59] Emma, V., Lo Nigro, S., Milone, C.: Nucl. Phys. A257, 438 (1976)
[60] Vinogradov, Yu.A., Kasilov, V.I., Lazareva, L.E., Nedorezov, V.G., Nikitina, N.V., Parovik, N.M., Ranyuk, Yu.N., Sorokin, P.V.: Sov. J. Nucl. Phys. 24, 357 (1976)
[61] di Napoli, V., Terranova, M.L., de Carvalho, H.G., Martins, J.B., Pinheiro Filho, J.D., Tavares, O.A.P.: J. Inorg. Nucl. Chem. 39, 1727 (1977)
[62] di Napoli, V., Salvetti, F., Terranova, M.L., de Carvalho, H.G., Martins, J.B., Tavares, O.A.P.: J. Inorg. Nucl. Chem. 40 175 (1978)
[63] Aleksandrov, B.M., Krivokhatskii, A.S., Kuznetsov, V.L., Lazareva, L.E., Nedorezov, V.G., Nikitina, N.V., Ranyuk, Yu.N.: Sov. J. Nucl. Phys. 28, 600 (1978)
[64] Gann, A.V., Nazarova, T.S., Noga, V.I., Ranyuk, Yu.N., Sorokin, P.V., Telegin, Yu.N.: Sov. J. Nucl. Phys. 30, 453 (1979)
[65] Martins, J.B., de Almeida, E.S., di Napoli, V., Foshina, M., Tavares, O.A.P., Terranova, M.L.: J. Inorg. Nucl. Chem. 43, 1115 (1981)
[66] Pinheiro Filho, J.D.: Doctoral Thesis, Centro Brasileiro de Pesquisas Fisicas, Rio de Janeiro (1983) (in português)
[67] Barashenkov, V.S., Gereghi, F.G., Iljinov, A.S., Jonsson, G.G., Toneev, V.D.: Nucl. Phys. A231, 462 (1974)
[68] Iljinov, A.S., Cherapanov, E.A., Chigrinov, S.E.: Sov. J. Nucl. Phys. 32, 166 (1980)
[69] Damashek, M., Gilman, F.J.: Phys. Rev. D1, 1319 (1970)
[70] Armstrong, T.A., Hogg, W.R., Lewis, G.M., Robertson, A.W., Brookes, G.R., Clough, A.S., Freeland, J.H., Galbraith, W., King, A.F., Rawlinson, W.R., Tait, N.R.S., Thompson, S.C., Tolfree, D.W.L.: Nucl. Phys. B41, 445 (1972)

[71] Rossi, P., De Sanctis, E., Levi Sandri, P., Bianchi, N., Guaraldo, C., Lucherini, V., Muccifora, V., Polli, E., Reolon, A.R., Urciuoli, G.M.: Phys. Rev. C40, 2412 (1989)
[72] Myers, H., Gomez, R., Guinier, D., Tollestrup A.V.: Phys. Rev. 121, 630 (1961)
[73] Tavares, O.A.P., Terranova, M.L.: J. Phys. G: Nucl. Part. Phys. 18, 521 (1992)
[74] Anghinolfi, M., Bianchi, N., Corvisiero, P., De Sanctis E., Frullani, S., Garibaldi, F., Gervino, G., Guaraldo, C., Levi Sandri, P., Lucherini, V., Muccifora, V., Polli, E., Reolon, A.R., Ricco, G., Ripani, M., Rossi, P., Sanzone, M., Taiuti, M., Urciuoli, M.G., Zucchiatti, A.: Laboratori Nazionali di Frascati-LNF/INFN Report 89/045 (1989)
[75] Anghinolfi, M., Bianchi, N., Corvisiero, P., Deppman, A., De Sanctis, E., Ebolese, A., Fantoni, A., Gervino, G., Levi Sandri, P., Lucherini, V., Mazzaschi, L., Mokeev, V., Muccifora, V., Polli, E., Reolon, A.R., Ricco, G., Ripani, M., Rossi, P., Sanzone, M., Taiuti, M., Zucchiatti, A.: Laboratori Nazionali di Frascati-LNF/INFN Report 91/089 (1991)
[76] Ahrens, J.: Nucl. Phys A446, 229c (1985)
[77] Ahrens, J., O'Connell, J.S.: Comm. Nucl. Part. Phys. 14, 245 (1985)
[78] de Almeida, E.S.: Doctoral Thesis, Centro Brasileiro de Pesquisas Fisicas, Rio de Janeiro, December 1979 (in portugûes).
[79] de Almeida, E.S., Foshina, M., di Napoli, V., Terranova, M.L.: J. Inorg. Nucl. Chem. 43, 2589 (1981)
[80] Foshina, M., Martins, J.B., Tavares O.A.P., di Napoli, V.: Radiochimica Acta 46, 57 (1989)
[81] Rudstam, G., Z. Naturforsch. 21a, 1027 (1966)
[82] Arakelyan, E.A., Balabekyan, A.R., Danagulyan, A.S., Khudaverdyan, A.G.: Sov. J. Nucl. Phys. 41, 533 (1985)
[83] Kasilov, V.I., Mitrofanova, A.V., Ranyuk, Yu.N., Sorokin, P.V., Sov. J. Nucl. Phys. 15, 228 (1972).